

cells, present pre-expansion, were not detectable after one month of culture. CD4⁺ CD25⁺ cells were intracellularly stained with anti-Foxp3 mAb (open) and isotype control (shaded). (C) IFN- γ , IL-2, IL-4, and IL-10 secretion of expanded TIL was determined by ELISPOT assays. Cytokine secretion by TIL from the breast cancer ascites specimen prior to expansion is shown as a control. Pre-expansion samples from melanoma and ovarian cancer specimens were not studied because of low initial cell numbers.
doi:10.1371/journal.pone.0030229.g004

cell-cell contact using the transwell assay (Figure 5B). A single stimulation, without any exogenously added cytokines, expanded CD8⁺ T cells by an average of 40.5% better when CD4⁺ T cells were present but separated from CD8⁺ T cells by the transwell membrane ($P < 0.005$). In co-cultures where CD4⁺ and CD8⁺ T cells were mixed, allowing for direct cell-cell contact, CD8⁺ T cells expanded more than in cultures where they were separated from CD4⁺ T cells by the transwell membrane ($P < 0.05$). These results suggest that observed CD4⁺ T cell help involves both soluble factors and cell-cell contact.

To identify molecules mediating the observed CD4⁺ T cell help, culture supernatants of CD4⁺/CD8⁺ T cell mixed and separate cultures were tested for a panel of soluble factors (Figure 5C and Table S1). Greater quantities of MIP-1 α , MIP-1 β , and RANTES were detected in CD4⁺/CD8⁺ T cell mixed cultures compared to separate cultures, suggesting increased production in mixed cultures. In contrast, IL-2 and IL-21, as well as IL-10, IL-17, TNF- α , and TNF- β , were detected at lower levels in mixed cultures, consistent with more consumption or less production of these cytokines.

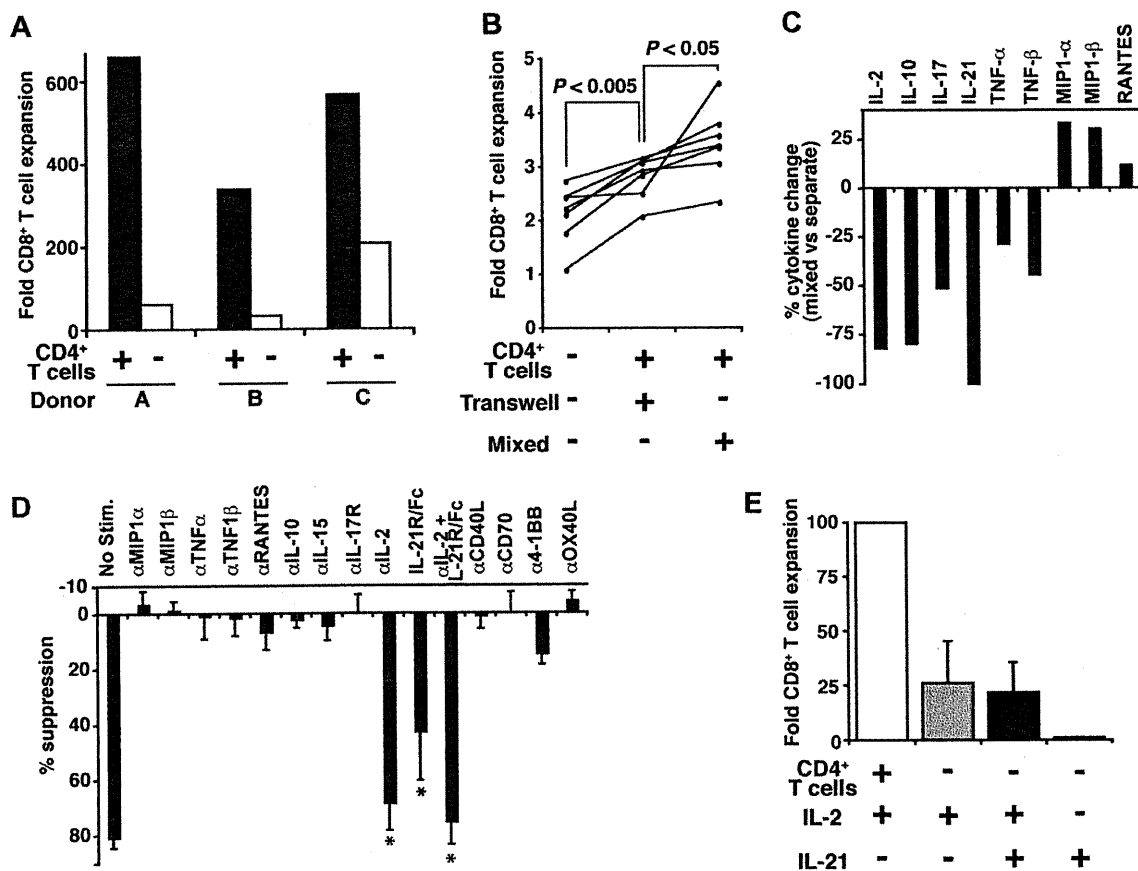


Figure 5. Autologous CD4⁺ T cell secretion of IL-2/IL-21 is necessary but not sufficient to help CD8⁺ T cells proliferate. (A) CD8⁺ T cells were stimulated twice by aAPC/mOKT3 with or without CD4⁺ T cells and treated with IL-2 between stimulations. Fold expansion of CD8⁺ T cells over 28 days is shown for 3 donors. (B) CD8⁺ T cells were stimulated only once by aAPC/mOKT3 with or without CD4⁺ T cells in transwell plates. No IL-2 or other cytokines were given. Fold expansion of CD8⁺ T cells over 6 days is shown for 7 donors. (C) Culture supernatants were tested for a panel of soluble factors to identify mediators of CD4⁺ T cell help. Relative changes in cytokines, comparing mixed vs. separate cultures, are shown. Data is representative of two donors. Absolute values for two donors are shown in Table S1. (D) Suppression of CD8⁺ T cell expansion in the presence of CD4⁺ T cells by blocking reagents is presented as percent suppression relative to control. Values indicate mean of four independent experiments; error bars show s.d. * $P < 0.005$. (E) CD8⁺ T cells were stimulated twice with aAPC/mOKT3 in the presence or absence of CD4⁺ T cells. IL-2, IL-21, or both were added in each condition. Fold expansion of CD8⁺ T cells over 28 days is shown. Percent expansion was calculated by dividing the number of expanded CD8⁺ T cells by the number of CD8⁺ T cells expanded in the presence of CD4⁺ T cells. Values indicate mean of six independent experiments; error bars show s.d.
doi:10.1371/journal.pone.0030229.g005

To differentiate between “more consumption” and “less production,” CD4⁺/CD8⁺ T cell mixed cultures were stimulated in the presence of blocking reagents, and suppression of CD8⁺ T cell expansion was assessed (Figure 5D). Blockade of IL-2 and IL-21 resulted in a reduction of expansion by 68.8% ($P < 0.005$) and 42.9% ($P < 0.005$), respectively. These results indicate that the decreased levels of IL-2 and IL-21 in CD4⁺/CD8⁺ T cell mixed cultures were due to more consumption rather than less production and that these cytokines may be necessary mediators of CD4⁺ T cell help in this human-based *in vitro* system. To test whether IL-2/IL-21 could substitute for the observed CD4⁺ T cell help, CD8⁺ T cells stimulated with aAPC/mOKT3 were supplemented with IL-2, IL-21, or both (Figure 5E). CD8⁺ T cells did not expand without IL-2. The addition of IL-2 with or without IL-21 did not improve CD8⁺ T cell expansion to the level observed when cocultured with CD4⁺ T cells, demonstrating that IL-2 plus IL-21 are not sufficient to replace CD4⁺ T cell help.

Exogenous IL-2/IL-21 and upregulation of IL-21 receptor can partially recapitulate CD4⁺ T cell help of CD8⁺ T cell expansion *in vitro*

Interestingly, we observed that higher expression of the IL-21 receptor (IL-21R) on CD8⁺ T cells occurred when CD4⁺ T cells were present during stimulation by aAPC/mOKT3 (Figure 6A).

Higher IL-21R expression on CD8⁺ T cells was not induced by supplementing cultures with IL-2 and IL-21 (data not shown). This prompted us to hypothesize that increased upregulation of IL-21R on CD8⁺ T cells is critical for the full effect of IL-21 secreted by CD4⁺ T cells. We constitutively expressed IL-21R on CD8⁺ T cells (Figure 6B, left) and stimulated them with aAPC/mOKT3 in the presence of IL-2/IL-21. In accordance with the transduction efficiency of IL-21R to 75.9%, CD8⁺ T cell proliferation partially increased to levels seen in the presence of CD4⁺ T cells (Figure 6B, right). This indicates that elevated expression of IL-21R is necessary and can partially recapitulate CD4⁺ T cell help for CD8⁺ T cell proliferation.

Discussion

A novel human cell-based aAPC expanded CD3⁺ T cells *in vitro* without the addition of allogeneic feeder PBMC. Phenotypic analysis of expanded healthy donor T cells and TIL showed, that while both CD4⁺ and CD8⁺ T cells expanded, CD8⁺ T cells predominated. In this model system, we demonstrated that CD8⁺ T cell expansion depended on the presence of CD4⁺ T cells, suggesting that CD4⁺ T cells provided help to proliferating CD8⁺ T cells. The CD4⁺ T cell secreted cytokines, IL-2 and IL-21, and the CD4⁺ T cell-dependent upregulation of IL-21R on CD8⁺ T cells were necessary for the observed CD4⁺ T cell help.

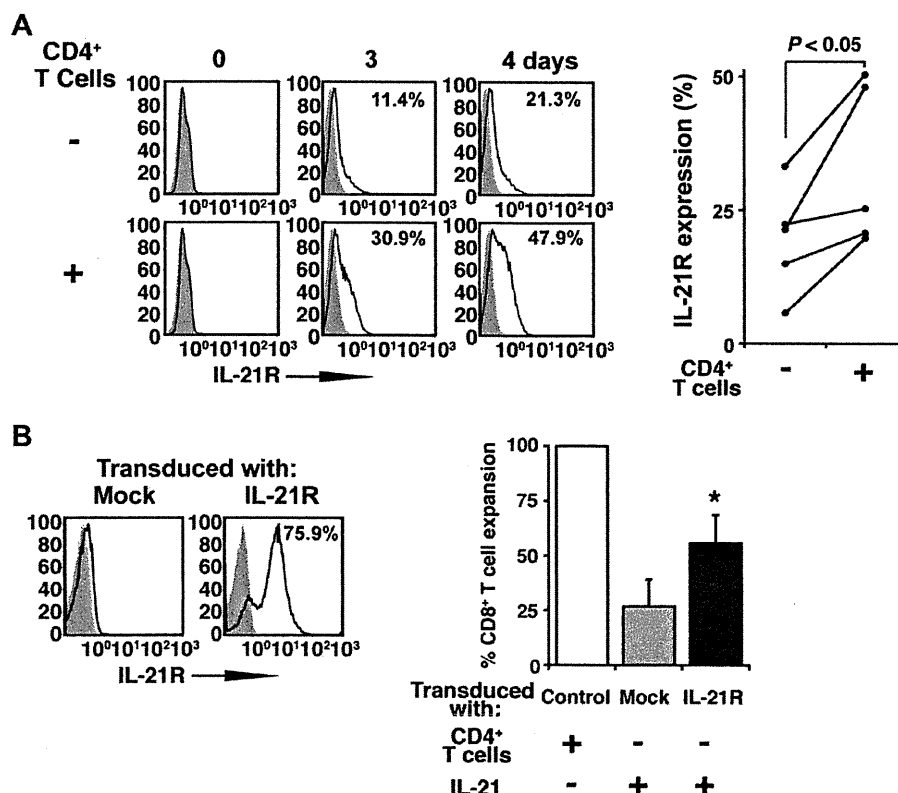


Figure 6. IL-2/IL-21 and upregulation of IL-21R expression replace CD4⁺ T cell help of CD8⁺ T cell expansion *in vitro*. (A) IL-21R expression on CD8⁺ T cells stimulated with aAPC/mOKT3 in the presence or absence of CD4⁺ T cells was studied by flow cytometry. On the left, histogram plots for 1 donor is shown and, on the right, IL-21R expression on day 4 is displayed for 5 donors. (B) IL-21R expression on CD8⁺ T cells ectopically transduced with mock or IL-21R is shown (left). Expansion of transduced CD8⁺ T cells stimulated twice by aAPC/mOKT3 with or without IL-21 is compared (right). Percent expansion was calculated by dividing the number of expanded transduced CD8⁺ T cells by that of CD8⁺ T cells stimulated in the presence of CD4⁺ T cells. Values indicate mean of four independent experiments; error bars show s.d. * $P < 0.005$. doi:10.1371/journal.pone.0030229.g006

IL-2 and IL-21 have previously been shown to mediate CD4⁺ T cell help in murine *in vivo* studies. IL-2, one of the few effector cytokines made by naïve CD4⁺ T cells, expands activated T cells and is essential in the development of CD8⁺ T cell memory responses to pathogens [60]. While CD8⁺ T cell responses during acute viral infections were relatively independent of IL-2, the development of protective CD8⁺ T cell memory responses required IL-2 exposure during priming [35–37]. *In vivo* models also indicate that IL-21 is critical for containing chronic viral infections and preventing the deletion of high affinity antiviral CD8⁺ T cells. IL-21 secretion by CD4⁺ T cells enables the generation, sustained proliferation, and maintenance of polyfunctional CD8⁺ T cells during chronic infection [39–41].

Our results confirmed a role for IL-2 and IL-21 in human CD4⁺ T cell help. By using a standardized aAPC, we were able to single out and examine the effects of cocultured CD4⁺ T cells, unhindered by immunostimulatory and inhibitory factors produced by allogeneic feeder cells. Stimulation of T cells with aAPC/mOKT3 induced the secretion of cytokines and chemokines, including high levels of interferon- γ , MIP-1 α , and MIP-1 β . Among all the cytokines and chemokines studied, blocking experiments identified IL-2 and IL-21 as necessary for CD4⁺ T cell help of CD8⁺ T cell expansion. These cytokines alone, however, were not sufficient to replace CD4⁺ T cells. We showed that CD4⁺ T cells help by enhancing IL-21R expression on CD8⁺ T cells, rendering them more responsive to secreted IL-21. Taken together, the secretion of IL-2/IL-21 and the induction of IL-21R are necessary and sufficient to partially recapitulate human CD4⁺ T cell help of CD8⁺ T cell expansion *in vitro*.

Transwell assays showed that the CD4⁺ T cell dependent expansion of CD8⁺ T cells was also mediated by cell-cell contact factors. CD40-CD40 ligand interactions have been shown to mediate CD4⁺ T cell help through CD40-mediated activation of dendritic cells, which are then “licensed” to stimulate CD8⁺ T cells [43,44,61]. CD40 ligation was also shown to increase IL-21R expression on B lymphocytes suggesting a mechanism for IL-21R upregulation on CD8⁺ T cells [62]. However, we did not observe any suppression of CD8⁺ T cell expansion following blockade of CD40 ligand (Figure 5D) even though expanded CD4⁺ T cells strongly expressed CD40 ligand (Figure 2C). Furthermore, stimulation with aAPC/mOKT3 in the presence of CD40 ligation and the addition of IL-21 did not consistently enhance CD8⁺ T cell expansion (data not shown). Therefore, these results are in agreement with others who have shown that CD4⁺ T cells do not provide direct help to CD8⁺ T cells through CD40 ligation [63,64]. It should be noted that blocking of CD70, 4-1BB, or OX40 signaling also did not suppress the expansion of CD8⁺ T cells in the presence of CD4⁺ T cells (Figure 5D).

aAPC induced polyclonal expansion of both CD4⁺ and CD8⁺ T cells as shown by the absence of clonal skewing of the TCR V β repertoire. The ability to further expand antigen-specific T cells capable of killing tumor targets indicated that the TCR repertoire for highly avid T cells was preserved. Also, expanded TIL secreted higher amounts of Th1 cytokines, IFN- γ and IL-2, which are associated with anti-tumor immunity. While aAPC/mOKT3 induced substantial expansion of CD8⁺ T cells in the presence of CD4⁺ T cell help, terminal effector T cell differentiation did not occur, as demonstrated by the central memory~effector memory phenotype (CD45RA⁺ CD45RO⁺ CD62L⁺). Retention of CD62L expression would enable homing to lymph nodes, where encounter with antigen presented by professional APC could augment immune responses [65]. CD27, which is down-regulated in late stage effector T cells, was also highly expressed. CD27 expression by *in vitro* expanded TIL and T cell clones has been

associated with persistence and clinical responses after adoptive transfer [56,57,59,66].

We also found that expanded T cells were not contaminated by cells with the CD4⁺ CD25⁺ Foxp3⁺ Treg phenotype even when CD4⁺ CD25⁺ Foxp3⁺ T cells were present prior to stimulation. We previously found that K562-based aAPC expressing HLA-DR molecules did not expand Foxp3⁺ cells even though aAPC itself produces modest amounts of the Treg cell growth factor TGF- β [48]. We previously reported that aAPC also secretes IL-6 [47]. It is possible that IL-6, secreted by aAPC, might interfere with Foxp3⁺ Treg cell expansion [67,68].

Adoptive transfer of *in vitro* expanded T cells has led to clinically significant anti-tumor responses in patients [30]. By leveraging autologous CD4⁺ T cell help, aAPC/mOKT3 eliminates the use allogeneic feeder cells for T cell expansion, potentially increasing the availability of adoptive therapy as a cancer treatment. We previously reported the development of K562-based aAPCs dedicated to the expansion of HLA-restricted antigen-specific CD4⁺ and CD8⁺ T cells [47,48]. Antigen-specific CD4⁺ and CD8⁺ T cells expanded *in vitro* with these aAPC had a central memory~effector memory phenotype (CD45RA⁺ CD62L⁺) and possessed surprisingly prolonged *in vitro* longevity without feeder cells or cloning. In a recent clinical trial, HLA-A2-restricted MART1 peptide-specific CD8⁺ T cells generated *in vitro* with aAPC were infused to advanced melanoma patients [69]. Without lymphodepletion or IL-2 administration, transferred T cells could persist for >16 months, established anti-tumor immunological memory *in vivo*, trafficked to tumor, and induced clinical responses. aAPC/mOKT3 extends the K562 platform to the stimulation of T cells regardless of HLA subtype. The aAPC/mOKT3-based T cell expansion system facilitates the understanding of mechanisms for human CD4⁺ T cell help and provides a novel strategy to expand T cells for *in vitro* and *in vivo* uses.

Materials and Methods

Ethics Statement

All specimens and clinical data were collected under protocols approved by the Institutional Review Board at the Dana-Farber Cancer Institute (DFCI). All patients provided written informed consent for the collection of samples and subsequent analysis.

cDNAs and cell lines

cDNAs encoding the heavy and light chains for a membranous form of anti-CD3 mAb (OKT3, mIgG2a) were cloned from hybridoma cells (ATCC, VA). HLA null K562 transduced with CD80 and CD83 has been described previously [47,53]. CD80⁺ CD83⁺ K562 cells were retrovirally transduced with the heavy and light chains of a membranous form of anti-CD3 mAb. After drug selection, anti-CD3 mAb expressing cells were isolated by magnetic bead guided sorting (Miltenyi Biotec, CA). High expression of a membranous form of anti-CD3 mAb on the cell surface was confirmed by flow cytometry. The parental cell line K562 lacks the endogenous expression of any HLA molecule, but does endogenously express the adhesion molecules CD54 and CD58.

Retrovirus supernatants expressing IL-21R was harvested from PG13 cells. Fresh CD8⁺ T cells purified from healthy donors were first activated with anti-CD3 (0.75 μ g/ml) and anti-CD28 (1 μ g/ml) mAbs (Fitzgerald Industries International, MA) for two days. Pre-activated T cells were infected with IL-21R or mock retrovirus supernatants every 24 hr at an MOI of 10 for 10 days and treated with 50 IU/ml IL-2 between infections. Following the assessment

of IL-21R expression by flow cytometry analysis, infected T cells were stimulated with aAPC/mOKT3.

T2, A375, and Malme-3M cell lines were obtained from ATCC as described elsewhere [47].

T cell expansion

Healthy donor PBMC were obtained by leukapheresis performed at the DFCI Kraft Family Blood Donor Center. Cells were isolated by Ficoll-Hypaque density gradient centrifugation and CD3⁺, CD4⁺, or CD8⁺ T cells were purified by negative selection via MACS sorting according to the manufacturer's protocol (Miltenyi Biotec, CA). TIL samples were processed by centrifugation of malignant ascites or mechanical and enzymatic digestion of melanoma metastases with collagenase as previously described [70]. CD3⁺ TIL were obtained by positive or negative selection via MACS sorting (Miltenyi Biotec, CA). aAPC/mOKT3 cells were irradiated (200 Gy) and added to purified T cells at a T cell to aAPC ratio of 20:1 unless otherwise noted. Dynabeads CD3/CD28 (Invitrogen, CA) were used as stimulators according to the manufacturer's instruction at a T cell to bead ratio of 1:3. Expanding T cells were cultured in RPMI 1640 containing 10% human AB sera and gentamycin (Invitrogen, CA), and between stimulations, unless otherwise noted, 300 IU/ml IL-2 (Prometheus, CA) was added every 3-4 days. In the absence of CD4⁺ T cells, CD8⁺ T cells expanded only in the presence of IL-2. Where indicated, 50 ng/ml IL-21 (Peprotech, NJ) was added every 3-4 days. Unless otherwise noted, T cells were restimulated every two weeks. Expanded cells were characterized two weeks after the second stimulation. Cell viability was >90% by trypan blue exclusion.

To test whether antigen-specific cultures can be generated from CD3⁺ T cells polyclonally expanded with aAPC/mOKT3, CD3⁺ T cells derived from HLA-A*0201 (A2)⁺ donors were initially stimulated and expanded with aAPC/mOKT3 for one month. Subsequently, CD8⁺ T cells were purified and further stimulated with Flu or MART1 peptide-pulsed aAPC/A2 as previously described [47,53].

Analysis of cultured T cells

Flow cytometry analysis was performed using mAbs for the following antigens: CD4, CD8, CD25, CD28, CD56, CD62L, and IL-2Rβ (Coulter, CA); CD40 ligand, CD80, IL-7Rα, OX40, OX40 ligand, and 4-1BB (BD Biosciences, CA); CD27, CD45RA, CD45RO and CD83 (Invitrogen, CA); CCR4 and CCR7 (R&D Systems, MN); ICOS, NKG2D, and PD-1 (eBioscience, CA); CD38, Foxp3, HLA-DR, and 4-1BB ligand (Biolegend, CA); CD40 and CD70 (Ancell, MN); IL-21R (R&D Systems, MN); or BD Biosciences, CA). Goat anti-mouse IgG (H+L) Fab (Jackson ImmunoResearch, PA) was used to detect surface expression of murine Ig. Assessment of TCR Vβ subfamily usage was performed using TCR Vβ mAbs (Beta Mark, Coulter, CA).

To assess the production/consumption of soluble factors in T cell cultures, purified CD4⁺, CD8⁺, or a 1:1 mixture of CD4⁺ and CD8⁺ T cells were stimulated with irradiated aAPC/mOKT3 for 72 hours and supernatants were measured for: GM-CSF, IFN-γ, IL-2, IL-4, IL-10, IL-12, IL-15, IL-17, MIP-1α, MIP-1β, RANTES, TNF-α, TNF-β, and TRAIL (R&D Systems, MN); IL-7 (Diaclone/Cell Sciences, MA); IL-18 (Medical & Biological Laboratories, Japan); and IFN-α (PBL Biomedical Laboratories, NJ). IL-21 (eBiosciences, CA) was measured at 48-hours. Relative changes in cytokines resulting from mixed cultures of CD4⁺ and CD8⁺ T cells vs. separate CD4⁺ and CD8⁺ T cell cultures were determined by the following formula: (x-y)/y, where x = cytokine secreted by CD4⁺ and CD8⁺ T cell mixed co-cultures and y is the

average of cytokine produced in separately stimulated CD4⁺ and CD8⁺ T cell cultures.

IFN-γ ELISPOT and standard chromium release assays were performed as described elsewhere [47,53]. IL-2, IL-4 and IL-10 ELISPOT assays were performed according to the manufacturer's protocol (R&D Systems, MN).

Transwell and blocking assays

Transwell assays were performed by placing purified CD4⁺, CD8⁺, or a mixture of CD4⁺ and CD8⁺ T cells into Millicell-24 plate chambers (Millipore) which were separated by a 0.4 μm filter allowing free movement of soluble factors but not cells. T cells were stimulated once with aAPC/mOKT3 in the absence of exogenous cytokines. Six days later, expansion of CD8⁺ T cells was determined.

Blocking assays were performed in 96-well round bottomed plates where CD4⁺ and CD8⁺ T cells were combined 1:1 and then stimulated with irradiated mOKT3/aAPC in the presence of blocking reagents. Blocking mAbs used recognized IL-2, IL-10, IL-15, IL-17R, MIP-1α, MIP-1β, OX40 ligand, RANTES, TNFα, and TNFβ (R&D Systems, MN); 4-1BB (Neomarkers, CA); CD40 ligand (Biolegend, CA); and CD70 (Ancell, MN). IL-21 was blocked using recombinant human IL-21R subunit/Fc chimeric protein (R&D Systems, MN) as previously described [71]. Six days later, CD8⁺ T cell expansion was determined.

Statistical analysis

Data analysis was performed using the paired, one-sided Student's t-test where $P < 0.05$ was considered to be statistically significant.

Supporting Information

Figure S1 K562-based aAPC/mOKT3, expressing a membranous form of anti-CD3 mAb, stimulates CD3⁺ T cell expansion. (A) CD3⁺ T cells were stimulated twice with aAPC/mOKT3 and supplemented with IL-2 at the following concentrations: 10 IU/ml (gray), 300 IU/ml (white) and 6,000 IU/ml (black). Fold expansion over 28 days is demonstrated. Without IL-2 addition, T cell expansion over the 28-day culture period was minimal. Data for three separate donors is shown. (B) CD3⁺ T cells were stimulated twice with aAPC/mOKT3 at the indicated aAPC: T cell ratios. Cultures were supplemented with IL-2 (300 IU/ml) between stimulations. Fold expansion of CD3⁺ T cells over one month is shown for two donors. (C) Phenotype of fresh healthy donor CD3⁺ T cells prior to stimulation is depicted to compare with the T cells shown in Figure 2C which were expanded with aAPC/mOKT3. Expression of surface molecules on gated CD4⁺ and CD8⁺ T cells is shown (open). Isotype mAb staining was used as a control (shaded). (D) HLA-A2⁺ healthy donor CD8⁺ T cells were stimulated with MART1 peptide-pulsed aAPC/A2 as previously described [47,53]. MART1 specific T cells were then stimulated twice with aAPC/mOKT3 in the presence of autologous CD4⁺ T cells. Fold expansion of MART1 T cells over one month is shown for three donors. (TIF)

Figure S2 TIL expanded with aAPC/mOKT3 express CD27 and CD28 and have a central memory~effector memory phenotype. CD3⁺ T cells from malignant ovarian ascites were stimulated twice with aAPC/mOKT3, and cultures were supplemented with IL-2 at 300 IU/ml. (A) Fresh, unstimulated TIL and (B) aAPC/mOKT3 expanded TIL were stained with indicated mAb (open) and isotype control (shaded).

TIL were analyzed after a one month expansion. Data depicted is on gated CD4⁺ and CD8⁺ T cells.
(TIF)

Table S1 Soluble factors in T cell cultures stimulated with aAPC/mOKT3. Concentrations of soluble factors (pg/ml) in supernatants of CD4⁺ separate, or CD8⁺ separate, and CD4⁺ and CD8⁺ mixed T cell cultures stimulated by aAPC/mOKT3 were measured by ELISA. ^aPercent change was calculated as

detailed in Methods. ^bnot applicable. Data from two different donors is depicted.
(DOC)

Author Contributions

Conceived and designed the experiments: MOB LMN NH. Performed the experiments: MOB OI MT SA AB GM MIM MMM APM NH. Analyzed the data: MOB LMN NH. Contributed reagents/materials/analysis tools: MOB OI YY MT SA HM LMN NH. Wrote the paper: MOB LMN NH.

References

- Dunn GP, Old LJ, Schreiber RD (2004) The immunobiology of cancer immunosurveillance and immunoeediting. *Immunity* 21: 137–148.
- Pellegrini M, Mak TW, Ohashi PS (2010) Fighting cancers from within: augmenting tumor immunity with cytokine therapy. *Trends Pharmacol Sci* 31: 356–363.
- Segal NH, Parsons DW, Peggs KS, Velculescu V, Kinzler KW, et al. (2008) Epitope landscape in breast and colorectal cancer. *Cancer Res* 68: 889–892.
- Parmiani G, De Filippo A, Novellino L, Castelli C (2007) Unique human tumor antigens: immunobiology and use in clinical trials. *J Immunol* 178: 1975–1979.
- Zhang L, Conejo-Garcia JR, Katsaros D, Gimotty PA, Massobrio M, et al. (2003) Intratumoral T cells, recurrence, and survival in epithelial ovarian cancer. *N Engl J Med* 348: 203–213.
- Marth C, Fiegl H, Zeimet AG, Muller-Holzner E, Deibl M, et al. (2004) Interferon-gamma expression is an independent prognostic factor in ovarian cancer. *Am J Obstet Gynecol* 191: 1598–1605.
- Kusuda T, Shigemasa K, Arihiro K, Fujii T, Nagai N, et al. (2005) Relative expression levels of Th1 and Th2 cytokine mRNA are independent prognostic factors in patients with ovarian cancer. *Oncol Rep* 13: 1153–1158.
- Mihm MC, Jr., Clemente CG, Cascinelli N (1996) Tumor infiltrating lymphocytes in lymph node melanoma metastases: a histopathologic prognostic indicator and an expression of local immune response. *Lab Invest* 74: 43–47.
- Mantovani A, Romero P, Palucka AK, Marincola FM (2008) Tumour immunity: effector response to tumour and role of the microenvironment. *Lancet* 371: 771–783.
- Curiel TJ, Coukos G, Zou L, Alvarez X, Cheng P, et al. (2004) Specific recruitment of regulatory T cells in ovarian carcinoma fosters immune privilege and predicts reduced survival. *Nat Med* 10: 942–949.
- Kobayashi N, Hiraoka N, Yamagami W, Ojima H, Kanai Y, et al. (2007) FOXP3+ regulatory T cells affect the development and progression of hepatocarcinogenesis. *Clin Cancer Res* 13: 902–911.
- Wilke CM, Wu K, Zhao E, Wang G, Zou W (2010) Prognostic significance of regulatory T cells in tumor. *Int J Cancer* 127: 748–758.
- Shimizu J, Yamazaki S, Sakaguchi S (1999) Induction of tumor immunity by removing CD25+CD4+ T cells: a common basis between tumor immunity and autoimmunity. *J Immunol* 163: 5211–5218.
- Sato E, Olson SH, Ahn J, Bundy B, Nishikawa H, et al. (2005) Intraepithelial CD8+ tumor-infiltrating lymphocytes and a high CD8+/regulatory T cell ratio are associated with favorable prognosis in ovarian cancer. *Proc Natl Acad Sci U S A* 102: 18538–18543.
- Gao Q, Qiu SJ, Fan J, Zhou J, Wang XY, et al. (2007) Intratumoral balance of regulatory and cytotoxic T cells is associated with prognosis of hepatocellular carcinoma after resection. *J Clin Oncol* 25: 2586–2593.
- Bolland CM, Gottschalk S, Leen AM, Weiss H, Straathof KC, et al. (2007) Complete responses of relapsed lymphoma following genetic modification of tumor-antigen presenting cells and T-lymphocyte transfer. *Blood* 110: 2838–2845.
- Dudley ME, Yang JC, Sherry R, Hughes MS, Royal R, et al. (2008) Adoptive cell therapy for patients with metastatic melanoma: evaluation of intensive myeloablative chemoradiation preparative regimens. *J Clin Oncol* 26: 5233–5239.
- Hunder NN, Wallen H, Cao J, Hendricks DW, Reilly JZ, et al. (2008) Treatment of metastatic melanoma with autologous CD4+ T cells against NY-ESO-1. *N Engl J Med* 358: 2698–2703.
- Mackensen A, Meidenbauer N, Vogl S, Laumer M, Berger J, et al. (2006) Phase I study of adoptive T-cell therapy using antigen-specific CD8+ T cells for the treatment of patients with metastatic melanoma. *J Clin Oncol* 24: 5060–5069.
- Peggs KS, Verfuert S, Pizzey A, Khan N, Guiver M, et al. (2003) Adoptive cellular therapy for early cytomegalovirus infection after allogeneic stem-cell transplantation with virus-specific T-cell lines. *Lancet* 362: 1375–1377.
- Berger C, Turtle CJ, Jensen MC, Riddell SR (2009) Adoptive transfer of virus-specific and tumor-specific T cell immunity. *Curr Opin Immunol* 21: 224–232.
- Morgan RA, Dudley ME, Wunderlich JR, Hughes MS, Yang JC, et al. (2006) Cancer regression in patients after transfer of genetically engineered lymphocytes. *Science* 314: 126–129.
- Pule MA, Savoldo B, Myers GD, Rossig C, Russell HV, et al. (2008) Virus-specific T cells engineered to coexpress tumor-specific receptors: persistence and antitumor activity in individuals with neuroblastoma. *Nat Med* 14: 1264–1270.
- Till BG, Jensen MC, Wang J, Chen EY, Wood BL, et al. (2008) Adoptive immunotherapy for indolent non-Hodgkin lymphoma and mantle cell lymphoma using genetically modified autologous CD20-specific T cells. *Blood* 112: 2261–2271.
- Lamers CH, Sleijfer S, Vulto AG, Kruit WH, Kliffen M, et al. (2006) Treatment of metastatic renal cell carcinoma with autologous T-lymphocytes genetically retargeted against carbonic anhydrase IX: first clinical experience. *J Clin Oncol* 24: e20–22.
- Kershaw MH, Westwood JA, Parker LL, Wang G, Eshhar Z, et al. (2006) A phase I study on adoptive immunotherapy using gene-modified T cells for ovarian cancer. *Clin Cancer Res* 12: 6106–6115.
- Dudley ME, Wunderlich JR, Yang JC, Sherry RM, Topalian SL, et al. (2005) Adoptive cell transfer therapy following non-myeloablative but lymphodepleting chemotherapy for the treatment of patients with refractory metastatic melanoma. *J Clin Oncol* 23: 2346–2357.
- Gattinoni L, Finkelstein SE, Klebanoff CA, Antony PA, Palmer DC, et al. (2005) Removal of homeostatic cytokine sinks by lymphodepletion enhances the efficacy of adoptively transferred tumor-specific CD8+ T cells. *J Exp Med* 202: 907–912.
- Klebanoff CA, Khong HT, Antony PA, Palmer DC, Restifo NP (2005) Sinks, suppressors and antigen presenters: how lymphodepletion enhances T cell-mediated tumor immunotherapy. *Trends Immunol* 26: 111–117.
- Rosenberg SA, Dudley ME (2009) Adoptive cell therapy for the treatment of patients with metastatic melanoma. *Curr Opin Immunol* 21: 233–240.
- Zhou J, Dudley ME, Rosenberg SA, Robbins PF (2005) Persistence of multiple tumor-specific T-cell clones is associated with complete tumor regression in a melanoma patient receiving adoptive cell transfer therapy. *J Immunother* 28: 53–62.
- Robbins PF, Dudley ME, Wunderlich J, El-Gamil M, Li YF, et al. (2004) Cutting edge: persistence of transferred lymphocyte clonotypes correlates with cancer regression in patients receiving cell transfer therapy. *J Immunol* 173: 7125–7130.
- Muranski P, Restifo NP (2009) Adoptive immunotherapy of cancer using CD4(+) T cells. *Curr Opin Immunol* 21: 200–208.
- Rochman Y, Spolski R, Leonard WJ (2009) New insights into the regulation of T cells by gamma(c) family cytokines. *Nat Rev Immunol* 9: 480–490.
- Wilson EB, Livingstone AM (2008) Cutting edge: CD4+ T cell-derived IL-2 is essential for help-dependent primary CD8+ T cell responses. *J Immunol* 181: 7445–7448.
- Bachmann MF, Wolint P, Walton S, Schwarz K, Oxenius A (2007) Differential role of IL-2R signaling for CD8+ T cell responses in acute and chronic viral infections. *Eur J Immunol* 37: 1502–1512.
- Williams MA, Tzysnik AJ, Bevan MJ (2006) Interleukin-2 signals during priming are required for secondary expansion of CD8+ memory T cells. *Nature* 441: 890–893.
- Bevan MJ (2004) Helping the CD8(+) T-cell response. *Nat Rev Immunol* 4: 595–602.
- Elsaesser H, Sauer K, Brooks DG (2009) IL-21 is required to control chronic viral infection. *Science* 324: 1569–1572.
- Yi JS, Du M, Zajac AJ (2009) A vital role for interleukin-21 in the control of a chronic viral infection. *Science* 324: 1572–1576.
- Frohlich A, Kisielow J, Schmitz I, Freigang S, Shamshiev AT, et al. (2009) IL-21R on T cells is critical for sustained functionality and control of chronic viral infection. *Science* 324: 1576–1580.
- Oh S, Perera LP, Terabe M, Ni L, Waldmann TA, et al. (2008) IL-15 as a mediator of CD4+ help for CD8+ T cell longevity and avoidance of TRAIL-mediated apoptosis. *Proc Natl Acad Sci U S A* 105: 5201–5206.
- Schoenberger SP, Toes RE, van der Voort EI, Offringa R, Melief CJ (1998) T-cell help for cytotoxic T lymphocytes is mediated by CD40-CD40L interactions. *Nature* 393: 480–483.
- Bennett SR, Carbone FR, Karamalis F, Flavell RA, Miller JF, et al. (1998) Help for cytotoxic-T-cell responses is mediated by CD40 signalling. *Nature* 393: 478–480.
- Walter EA, Greenberg PD, Gilbert MJ, Finch RJ, Watanabe KS, et al. (1995) Reconstitution of cellular immunity against cytomegalovirus in recipients of allogeneic bone marrow by transfer of T-cell clones from the donor. *N Engl J Med* 333: 1038–1044.
- Haque T, Wilkie GM, Jones MM, Higgins CD, Urquhart G, et al. (2007) Allogeneic cytotoxic T-cell therapy for EBV-positive posttransplantation lymphoproliferative disease: results of a phase 2 multicenter clinical trial. *Blood* 110: 1123–1131.

47. Butler MO, Lee JS, Ansen S, Neuberg D, Hodi FS, et al. (2007) Long-lived antitumor CD8⁺ lymphocytes for adoptive therapy generated using an artificial antigen-presenting cell. *Clin Cancer Res* 13: 1857–1867.
48. Butler MO, Ansen S, Tanaka M, Imataki O, Berzovskaya A, et al. (2010) A panel of human cell-based artificial APC enables the expansion of long-lived antigen-specific CD4⁺ T cells restricted by prevalent HLA-DR alleles. *Int Immunol* 22: 863–873.
49. Numbenjapon T, Serrano LM, Singh H, Kowolik CM, Olivares S, et al. (2006) Characterization of an artificial antigen-presenting cell to propagate cytolytic CD19-specific T cells. *Leukemia* 20: 1889–1892.
50. Suhoski MM, Golovina TN, Aquí NA, Tai VC, Varela-Rohena A, et al. (2007) Engineering artificial antigen-presenting cells to express a diverse array of costimulatory molecules. *Mol Ther* 15: 981–988.
51. Maus MV, Thomas AK, Leonard DG, Allman D, Addya K, et al. (2002) Ex vivo expansion of polyclonal and antigen-specific cytotoxic T lymphocytes by artificial APCs expressing ligands for the T-cell receptor, CD28 and 4-1BB. *Nat Biotechnol* 20: 143–148.
52. Dudley ME, Wunderlich JR, Shelton TE, Even J, Rosenberg SA (2003) Generation of tumor-infiltrating lymphocyte cultures for use in adoptive transfer therapy for melanoma patients. *J Immunother* 26: 332–342.
53. Hirano N, Butler MO, Xia Z, Ansen S, von Bergwelt-Baildon MS, et al. (2006) Engagement of CD83 ligand induces prolonged expansion of CD8⁺ T cells and preferential enrichment for antigen specificity. *Blood* 107: 1528–1536.
54. Prazma CM, Yazawa N, Fujimoto Y, Fujimoto M, Tedder TF (2007) CD83 expression is a sensitive marker of activation required for B cell and CD4⁺ T cell longevity in vivo. *J Immunol* 179: 4550–4562.
55. Levine BL, Bernstein WB, Connors M, Craighead N, Lindsten T, et al. (1997) Effects of CD28 costimulation on long-term proliferation of CD4⁺ T cells in the absence of exogenous feeder cells. *J Immunol* 159: 5921–5930.
56. Powell DJ, Jr., Dudley ME, Robbins PF, Rosenberg SA (2005) Transition of late-stage effector T cells to CD27⁺ CD28⁺ tumor-reactive effector memory T cells in humans after adoptive cell transfer therapy. *Blood* 105: 241–250.
57. Ochsenbein AF, Riddell SR, Brown M, Corey L, Baerlocher GM, et al. (2004) CD27 expression promotes long-term survival of functional effector-memory CD8⁺ cytotoxic T lymphocytes in HIV-infected patients. *J Exp Med* 200: 1407–1417.
58. Zhou J, Shen X, Huang J, Hodes RJ, Rosenberg SA, et al. (2005) Telomere length of transferred lymphocytes correlates with in vivo persistence and tumor regression in melanoma patients receiving cell transfer therapy. *J Immunol* 175: 7046–7052.
59. Huang J, Kerstann KW, Ahmadzadeh M, Li YF, El-Gamil M, et al. (2006) Modulation by IL-2 of CD70 and CD27 expression on CD8⁺ T cells: importance for the therapeutic effectiveness of cell transfer immunotherapy. *J Immunol* 176: 7726–7735.
60. Waldmann TA (2006) The biology of interleukin-2 and interleukin-15: implications for cancer therapy and vaccine design. *Nat Rev Immunol* 6: 595–601.
61. Ridge JP, Di Rosa F, Matzinger P (1998) A conditioned dendritic cell can be a temporal bridge between a CD4⁺ T-helper and a T-killer cell. *Nature* 393: 474–478.
62. de Toter D, Meazza R, Zupo S, Cutrona G, Matis S, et al. (2006) Interleukin-21 receptor (IL-21R) is up-regulated by CD40 triggering and mediates proapoptotic signals in chronic lymphocytic leukemia B cells. *Blood* 107: 3708–3715.
63. Lee BO, Hartson L, Randall TD (2003) CD40-deficient, influenza-specific CD8 memory T cells develop and function normally in a CD40-sufficient environment. *J Exp Med* 198: 1759–1764.
64. Sun JC, Bevan MJ (2004) Cutting edge: long-lived CD8 memory and protective immunity in the absence of CD40 expression on CD8 T cells. *J Immunol* 172: 3385–3389.
65. Gattinoni L, Klebanoff CA, Palmer DC, Wrzesinski C, Kerstann K, et al. (2005) Acquisition of full effector function in vitro paradoxically impairs the in vivo antitumor efficacy of adoptively transferred CD8⁺ T cells. *J Clin Invest* 115: 1616–1626.
66. Huang J, Khong HT, Dudley ME, El-Gamil M, Li YF, et al. (2005) Survival, persistence, and progressive differentiation of adoptively transferred tumor-reactive T cells associated with tumor regression. *J Immunother* 28: 258–267.
67. Korn T, Bettelli E, Oukka M, Kuchroo VK (2009) IL-17 and Th17 Cells. *Annu Rev Immunol* 27: 485–517.
68. Li MO, Flavell RA (2008) Contextual regulation of inflammation: a duet by transforming growth factor-beta and interleukin-10. *Immunity* 28: 468–476.
69. Butler M, Friedlander P, Mooney M, Drury L, Metzler M, et al. (2009) Establishing CD8⁺ T Cell Immunity by Adoptive Transfer of Autologous, IL-15 Expanded, Anti-Tumor CTL with a Central/Effector Memory Phenotype Can Induce Objective Clinical Responses. *Blood (ASH Annual Meeting Abstracts)* 114: 782.
70. Soiffer R, Lynch T, Mihm M, Jung K, Rhuda C, et al. (1998) Vaccination with irradiated autologous melanoma cells engineered to secrete human granulocyte-macrophage colony-stimulating factor generates potent antitumor immunity in patients with metastatic melanoma. *Proc Natl Acad Sci U S A* 95: 13141–13146.
71. Andersson AK, Feldmann M, Brennan FM (2008) Neutralizing IL-21 and IL-15 inhibits pro-inflammatory cytokine production in rheumatoid arthritis. *Scand J Immunol* 68: 103–111.

Expression of myeloperoxidase and gene mutations in AML patients with normal karyotype: double *CEBPA* mutations are associated with high percentage of MPO positivity in leukemic blasts

Shinya Tominaga-Sato · Hideki Tsushima · Koji Ando · Hidehiro Itonaga · Yoshitaka Imaizumi · Daisuke Imanishi · Masako Iwanaga · Jun Taguchi · Takuya Fukushima · Shinichiro Yoshida · Tomoko Hata · Yuki Yoshi Moriuchi · Kazutaka Kuriyama · Hiroyuki Mano · Masao Tomonaga · Yasushi Miyazaki

Received: 22 March 2011 / Revised: 23 May 2011 / Accepted: 23 May 2011 / Published online: 16 June 2011
© The Japanese Society of Hematology 2011

Abstract The percentage of myeloperoxidase (MPO)-positive blast cells is a simple and highly significant prognostic factor in AML patients. It has been reported that the high MPO group (MPO-H), in which >50% of blasts are MPO activity positive, is associated with favorable karyotypes, while the low MPO group (≤50% of blasts are MPO activity positive, MPO-L) is associated with adverse karyotypes. The MPO-H group shows better survival even when restricted to patients belonging to the intermediate chromosomal risk group or those with a normal karyotype. It has recently been shown that genotypes defined by the mutational status of *NPM1*, *FLT3*, and *CEBPA* are associated with treatment outcome in patients with cytogenetically normal AML. In this study, we aimed to evaluate the relationship between MPO positivity and gene mutations found in normal karyotypes. Sixty AML patients with normal karyotypes were included in this study. Blast cell

MPO positivity was assessed in bone marrow smears stained for MPO. Associated genetic lesions (the *NPM1*, *FLT3*-ITD, and *CEBPA* mutations) were studied using nucleotide sequencing. Thirty-two patients were in the MPO-L group, and 28 patients in the MPO-H group. *FLT3*-ITD was found in 11 patients (18.3%), *NPM1* mutations were found in 19 patients (31.7%), and *CEBPA* mutations were found in 11 patients (18.3%). In patients with *CEBPA* mutations, the carrying two simultaneous mutations (*CEBPA*^{double-mut}) was associated with high MPO expression, while the mutant *NPM1* without *FLT3*-ITD genotype was not associated with MPO activity. Both higher MPO expression and the *CEBPA*^{double-mut} genotype appeared to be associated with improved overall survival after intensive chemotherapy. Further studies are required to determine the importance of blast MPO activity as a prognostic factor, especially in *CEBPA* wild-type patients with a normal karyotype.

S. Tominaga-Sato · H. Itonaga · M. Iwanaga · J. Taguchi · Y. Miyazaki
Department of Hematology and Molecular Medicine Unit,
Atomic Bomb Disease Institute,
Nagasaki University Graduate School of Biomedical Sciences,
Nagasaki, Nagasaki, Japan

H. Tsushima (✉) · Y. Imaizumi · D. Imanishi · T. Fukushima · T. Hata
Department of Hematology,
Nagasaki University Hospital,
1-7-1 Sakamoto, Nagasaki 852-8501, Japan
e-mail: tsushima@nagasaki-u.ac.jp

K. Ando · S. Yoshida
Department of Internal Medicine,
Nagasaki National Medical Center,
Ohmura, Nagasaki, Japan

Y. Moriuchi
Division of Hematology,
Sasebo City General Hospital,
Sasebo, Nagasaki, Japan

K. Kuriyama
School of Health Sciences,
University of the Ryukyus, Okinawa,
Nishihara, Japan

H. Mano
Division of Functional Genomics,
Jichi Medical University, Shimotsuke, Tochigi, Japan

M. Tomonaga
Department of Hematology,
Japanese Red-Cross Nagasaki Atomic Bomb Hospital,
Nagasaki, Nagasaki, Japan

Keywords Acute myeloid leukemia · Normal karyotype · Myeloperoxidase · *CEBPA* mutations

1 Introduction

The AML87, -89, and -92 studies conducted by Japan Adult Leukemia Study Group (JALSG) revealed that patient age, ECOG performance status, leukocyte count, FAB subclass, the number of induction courses required to achieve complete remission (CR), the presence of good prognostic chromosomal abnormalities [t(8;21) or inv(16)], and percentage of myeloperoxidase (MPO)-stained positive blast cells at diagnosis were significant risk factors for overall survival (OS) of patients with acute myeloid leukemia (AML) [1]. In more recent AML201 study, it was shown that significant unfavorable prognostic features for OS were adverse cytogenetic risk group [2], age of more than 50 years, WBC more than $20 \times 10^9/L$, FAB classification of either M0, M6, or M7, and MPO-positive blasts less than 50% [3]. These observations imply that the percentage of MPO-positive blast cells is one of the important prognostic markers along with cytogenetics and molecular genetic information.

MPO, a microbicidal protein, is considered to be a golden marker for the diagnosis of AML in the French-American-British (FAB) and WHO classifications [4, 5]. In our previous reports [6–8], AML patients with a high percentage of MPO-positive blasts (>50% of blasts are MPO activity positive, MPO-H) had a significantly better complete remission (CR) rate, disease-free survival, and overall survival compared with the low MPO activity positive blast group ($\leq 50\%$ of blasts are MPO activity positive, MPO-L). Most patients with a favorable chromosomal risk profile were in the MPO-H group, and most of the patients with an adverse chromosomal risk profile were in the MPO-L group. The difference in OS between the low and high MPO groups was still observed in a cohort of patients with normal karyotypes, suggesting that MPO is highly expressed in the leukemic blasts of AML patients with a favorable prognosis. To fully understand this phenomenon, it would be important to analyze genetic factors associated with MPO expression, especially in patients with a normal karyotype.

In the WHO classification, mutations of *FLT3*, *NPM1* and *CEBPA* have been emphasized to have prognostic significance in AML patients with normal karyotype. The nucleophosmin 1 gene (*NPM1*) has been shown to be mutated in 45–64% of AML cases with a normal karyotype [9, 10], and *NPM1* mutations are associated with a favorable prognosis in the absence of the internal tandem duplication (ITD) type of fms-related tyrosine kinase-3 gene (*FLT3*) mutation, a known adverse prognostic factor

[11]. The CCAAT/enhancer binding protein- α gene (*CEBPA*) is another gene that has been shown to be mutated in AML patients with a normal karyotype [12, 13]. Mutations in the *CEBPA* gene are found in 5–14% of all AML cases and are associated with a relatively favorable outcome, and hence, have gained interest as a prognostic marker [14]. Recently, it has been shown that most AML patients with *CEBPA* mutations carry 2 simultaneous mutations (*CEBPA*^{double-mut}), whereas single mutations (*CEBPA*^{single-mut}) are less common. In addition it was found that the *CEBPA*^{double-mut} genotype is associated with a favorable overall and event-free survival [15, 16]. It is still unclear why *CEBPA*^{double-mut} AML patients have better outcomes than those with a single heterozygous mutation.

In this study, we retrospectively examined 60 de novo adult AML patients with normal karyotypes in order to obtain a better insight into the relationships between MPO positivity and other prognostic factors (*NPM1*, *FLT3*, and *CEBPA* mutations). In line with previous reports, both high MPO positivity in AML blasts and the *CEBPA*^{double-mut} genotype appeared to be associated with a favorable outcome, and it appeared that it was the *CEBPA*^{double-mut} genotype that associated with high blast MPO activity.

2 Materials and methods

2.1 Patients and treatments

The study population included 60 patients with newly diagnosed de novo AML that had been treated at the Department of Internal Medicine, Nagasaki National Medical Center, between 1990 and 2010. All patients had normal karyotype AML. AML was diagnosed according to the FAB classification. Two members independently assessed the percentage of MPO-positive blast cells in MPO-stained bone marrow smears. The main biological and clinical features of the patients are shown in Table 1. Excluding the 25 patients who did not receive conventional induction chemotherapy, all patients were treated according to the Japan Adult Leukemia Study Group (JALSG) protocols (AML89, -92, -95, -97, and -201 studies) [3, 17–19]. CR was determined as when blasts accounted for less than 5% of the cells in normocellular bone marrow with normal peripheral neutrophil and platelet counts. This study was approved by the Ethical Committees of the participating hospitals.

2.2 Analysis of the *FLT3*, *NPM1*, and *CEBPA* genes

High molecular weight genomic DNA was extracted from bone marrow and peripheral blood samples after Ficoll

Table 1 Characteristics of de novo AML patients with a normal karyotype

	All patients (<i>n</i> = 60)	Patients who received intensive chemotherapy (<i>n</i> = 36)
Median age (range) (year)	59.5 (15–81)	49 (15–67)
Male/female	32/28	18/18
FAB type		
M0	5	3
M1	10	5
M2	21	14
M4	18	11
M5	3	1
M6	3	2
M7	0	0
WBC (×10 ⁹ /L), median (range)	14.9 (0.7–556)	13.0 (0.7–246)
Performance status		
0–2	55	34
3–4	5	2
LDH (IU/L), median (range)	296 (120–5,325)	291 (140–2,606)
MPO		
Low (≤50%)	32	20
High (>50%)	28	16

FAB French–American–British, WBC white blood cells, LDH lactate dehydrogenase, MPO myeloperoxidase

separation of mononucleated cells (35 and 4 patients, respectively) using the QIAamp DNA Mini Kit (Qiagen, Hilden, Germany). In addition, we isolated genomic DNA from the BM smears of the AML patients (21 samples) using the QIAamp DNA blood Mini Kit (Qiagen, Hilden, Germany).

Mutations in the *FLT3*, *NPM1*, and *CEBPA* genes were detected by genomic DNA PCR and direct sequencing. Exons 14 and 15 and the intervening intron of the *FLT3* gene were amplified from DNA using the previously described primers FLT3-11F and FLT3-12R [20]. PCR for *NPM1* exon 12 was performed with genomic DNA, the same reagent, and the published primer molecules NPM1-F and NPM1-R [21]. PCR for *CEBPA* was performed using 2 overlapping primer pairs: CEBPA-CT3F (5'-TGCCGGGTATAAAA-GCTGGG-3') and CT3R (5'-CTCGTTGCTGTTCTTGTCCA-3'), CEBPA-PP2F (5'-TGCCGGGT-ATAAAGCTGGG-3') and PP2R (5'-CACGGTCTGGGCAAGCCTCGAGAT-3'). The PCR reactions were run in a final volume of 50 µL containing 10 ng DNA, 5× buffer, 0.2 mmol/L of each deoxynucleotide triphosphate, primers (0.3 µmol/L of each), nucleotides (0.2 mmol/L of each), and 1 U of KOD-Plus-Neo polymerase (TOYOBO, Osaka, Japan). The

mixture was initially heated at 94°C for 2 min, before being subjected to 35 cycles of denaturation at 94°C for 10 s and annealing and extension at 68°C for 1 min. The amplified products were cut out from a 1.2% agarose gel and purified with the MinElute Gel extraction kit (QIAGEN, Germany). To screen for mutations, the PCR products were sequenced in both directions with the following primers: FLT3-11F, FLT3-12R, NPM1-F, NPM1-R, CEBPA-CT1F, CEBPA-1R, CEBPA-PP2F, CEBPA-PP2R, CEBPA-2F (5'-GCTGGGCGGCATCTGCG-A-3'), and CEBPA-1R (5'-TGT-GCTGGAACAGGTCGGCCA-3') using a BigDye Terminator v3.1 Cycle Sequencing Kit and the ABI Prism 3100 ×1 Genetic Analyzer (Applied Biosystems, CA, USA). In the case of *NPM1* and *CEBPA* genes, when heterozygous data were identified by sequence screening, mutations were confirmed by cloning with the StrataClone Blunt PCR Cloning Kit (Stratagene, CA, USA) according to the manufacturer's recommendations. Four to ten recombinant colonies were chosen and cultured in LB medium. Plasmid DNA was prepared using a QIAprep spin plasmid miniprep kit (Qiagen, Hilden, Germany), and both strands were sequenced using the T3 and T7 primers and the CEBPA-2F and CEBPA-1R primers.

2.3 Statistical methods

To evaluate the relationship between the frequency of mutations status and clinical characteristics, the following variables were included in the analysis: age, FAB classification, peripheral WBC count, MPO-positivity rate, JALSG score [1], and CR achievement. A comparison of frequencies was performed using Fisher's exact test. Differences in percentage of MPO-positive blasts among patients with different mutational status of genes were compared using the non-parametric Kruskal–Wallis test and followed by Dunn's multiple comparison post-test. Overall survival (OS) was calculated using the Kaplan–Meier method [22], and the group differences were compared using the log-rank test. Thirteen patients who underwent allogeneic or autologous hematopoietic stem cell transplantation were not censored at the time of transplantation. For all analyses, statistical significance was considered at the level of two-tailed 0.05.

3 Results

3.1 Patients' characteristics

As shown in Table 1, the series included 60 patients. Their median age was 59.5 (15–81 years), and there were 32 males (53.3%) and 28 females (46.7%). All patients had normal cytogenetics. Using the percentage of MPO-positive leukemic blasts, as judged from bone marrow slides, the cases

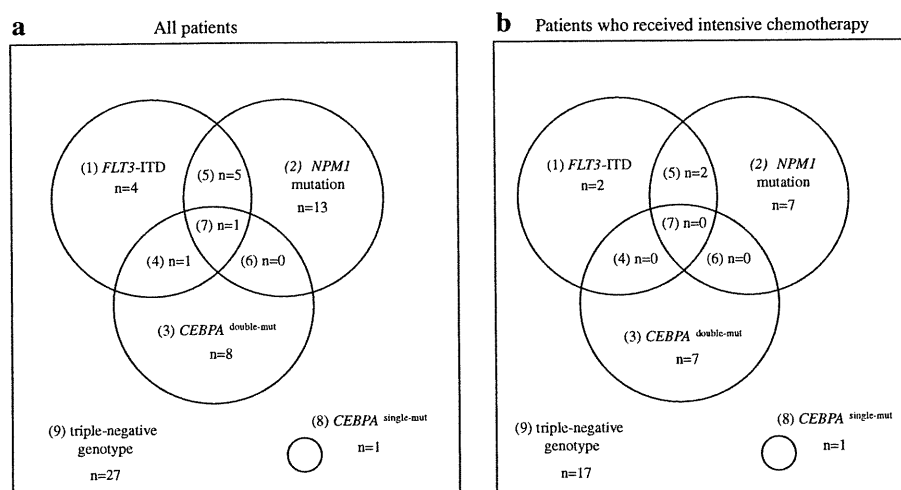


Fig. 1 Frequency and overlapping patterns of AML patients with a normal karyotype. Data are shown for all patients (**a**) and for patients who received intensive chemotherapy (**b**). **a** (1) *FLT3*-ITD + wt *NPM1* + wt *CEBPA* ($n = 4$, 6.7%), (2) wt *FLT3* + *NPM1* mutation + wt *CEBPA* ($n = 13$, 21.7%), (3) wt *FLT3* + wt *NPM1* + *CEBPA*^{double-mut} ($n = 8$, 13.3%), (4) *FLT3*-ITD + wt *NPM1* + *CEBPA*^{double-mut} ($n = 1$, 1.7%), (5) *FLT3*-ITD + *NPM1* mutation + wt *CEBPA* ($n = 5$, 8.3%), (6) wt *FLT3* + *NPM1* mutation + *CEBPA*^{double-mut} ($n = 0$, 0%), (7) *FLT3*-ITD + *NPM1* mutation + *CEBPA*^{double-mut} ($n = 1$, 1.7%), (8) wt *FLT3* + wt

NPM1 + *CEBPA*^{single-mut} ($n = 1$, 1.7%), (9) triple-negative genotype ($n = 27$, 45%). **b** (1) *FLT3*-ITD + wt *NPM1* + wt *CEBPA* ($n = 2$, 5.6%), (2) wt *FLT3* + *NPM1* mutation + wt *CEBPA* ($n = 7$, 19.4%), (3) wt *FLT3* + wt *NPM1* + *CEBPA*^{double-mut} ($n = 7$, 19.4%), (4) *FLT3*-ITD + wt *NPM1* + *CEBPA*^{double-mut} ($n = 0$, 0%), (5) *FLT3*-ITD + *NPM1* mutation + wt *CEBPA* ($n = 2$, 5.6%), (6) wt *FLT3* + *NPM1* mutation + *CEBPA*^{double-mut} ($n = 0$, 0%), (7) *FLT3*-ITD + *NPM1* mutation + *CEBPA*^{double-mut} ($n = 0$, 0%), (8) wt *FLT3* + wt *NPM1* + *CEBPA*^{single-mut} ($n = 0$, 0%), (9) triple-negative genotype ($n = 17$, 47.2%). wt wild-type

were divided into the High group (MPO-positive blasts > 50%) and Low group (MPO-positive blasts ≤ 50%). Thirty-two patients were classified into the Low group, and 28 patients were classified into the High group.

3.2 Mutational analysis

FLT3-ITD was found in 11 patients (18.3%), *NPM1* mutations were found in 19 patients (31.7%), and *CEBPA* mutations were found in 11 patients (18.3%). Frequency and an overlapping pattern of mutations are shown in Fig. 1. Among the patients with *CEBPA* mutations, approximately 90% (10 of 11 patients) of the patients had two *CEBPA* mutations (*CEBPA*^{double-mut}), whereas 10% (1 of 11 patients) had a single mutation. As previously reported, the mutations in the *CEBPA*^{double-mut} patients were clustered in the N- and C-terminal hotspots (Table 2; Fig. 2). *FLT3*-ITD mutation was associated with a higher WBC at the time of diagnosis, as reported previously. Neither *NPM1* nor *CEBPA* mutation status displayed a significant association with age, PS, WBC, FAB subtype, JALSG score, or CR achievement (Table 3).

3.3 Clinical outcome

OS was analyzed only in patients who received intensive chemotherapy ($n = 36$). They received chemotherapy

based on the treatment protocol described in the JALSG AML89, -92, -95, -97, and -201 studies. As reported previously [6], we observed an association between the percentage of MPO-positive blasts and the survival rate in the normal karyotype patients treated with intensive chemotherapy, although the significance in this cohort was rather low ($P = 0.10$) (Fig. 3). Figure 4 shows Kaplan–Meier curves according to genotype. ‘Other genotypes’ included the *FLT3*-ITD genotype, the *CEBPA*^{single-mut} genotype, and the triple-negative genotype consisting of the wild-type *NPM1* and *CEBPA* genotypes without *FLT3*-ITD. In line with previous reports [14], the patients with the *CEBPA*^{double-mut} genotype tended to show higher survival rate compared with patients displaying other genotypes ($P = 0.07$). In this study, the mutant *NPM1* without *FLT3*-ITD genotype was not significantly associated with treatment outcome, possibly due to the small number of patients.

3.4 Difference of MPO-positivity rate by gene mutation status

Figure 5 shows the level of the percentage of MPO-positive blasts by gene mutational status of the *CEBPA*, *FLT3*-ITD, and *NPM1*. The MPO-positivity rate was very high, over 50% (median 96, range 71–100), in all *CEBPA*^{double-mut} cases, but it was 20% in one case displaying the

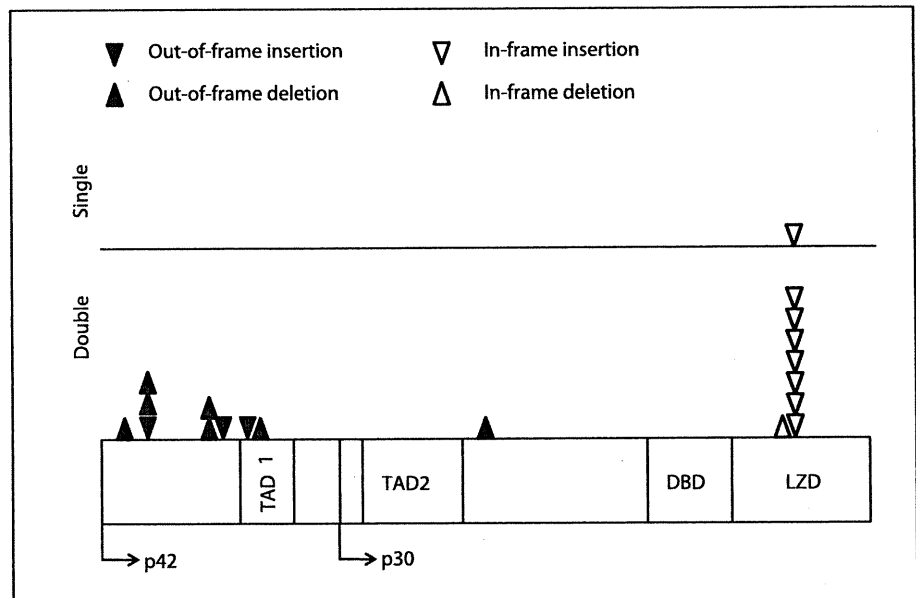
Table 2 Genetic findings of the patients with *CEBPA* mutations

Patient	Category	Nucleotide changes	Amino acid changes	Comments
4	Double	218_219insC 1129_1130insATGTGGAGACGCAGCAGAAAGGTGCTGGAGCTG ACCAGTGACAATGACCGCCTGCGCAAGC	P23fsX107 K326_327insHVETQQKVLELTSDNDRLRKR	Produces N-terminal stop codon In-frame insertion in bZIP
6	Double	200_218delinsCT 1087_1089dup	S16fsX101 K313dup	Produces N-terminal stop codon In-frame duplication in bZIP
7	Double	368_369insA 1080_1082del	A72fsX107 T310_Q311del	Produces N-terminal stop codon In-frame deletion in bZIP
13	Double	303_316del 1062_1063insTTG	P50fsX102 K304_Q305insV	Produces N-terminal stop codon In-frame insertion in bZIP
19	Double	215_225del 1101_1102insCAGCGCAACGTGGAGACGCAGCAGAA AGGTGCTGGAGCTG	P21fsX103 L317_T318insQRNVETQQKVLEL	Produces N-terminal stop codon In-frame insertion in bZIP
22	Double	213del 1064_1129dup	P22fsX159 K304_Q305insQRNVETQQKVLELTSDNDRLRKR	Produces N-terminal stop codon In-frame insertion in bZIP
27	Double	324_328dup 1062_1063insTTG	E59fsX161 K304_Q305insV	Produces N-terminal stop codon In-frame insertion in bZIP
39	Double	213del 1081_1086dup	P22fsX159 Q311_Q312dup	Produces N-terminal stop codon In-frame duplication in bZIP
47	Double	397del 1101_1102insCAGCGCAACGTGGAGACGCAGCA GAAGGTGCTGGAGCTG	F82fsX159 L317_T318insQRNVETQQKVLEL	Produces N-terminal stop codon In-frame insertion in bZIP
49	Double	297_304del 758del	A48fsX104 A202fsX317	Produces N-terminal stop codon Frameshift between TAD2 and bZIP; produces stop codon in bZIP
35	Single	1087_1089dup	K313dup	In-frame duplication in bZIP

Nucleotide numbering was performed according to NCBI Entrez accession no. XM_009180.3, in which the major translational start codon starts at nucleotide position 151. The locations of functional domains are derived from Mueller and Pabst.1

bZIP basic leucine zipper region, *TAD2* second transactivation domain

Fig. 2 Location of mutations detected in the *CEBPA*^{single-mut} and *CEBPA*^{double-mut} patients. Transactivation domain (TAD) 1, amino acids (AA) 70–97; p30 ATG, AA120; TAD2, AA 126–200; DNA-binding domain (DBD), AA 278–306; leucine zipper domain (LZD), AA 307–358



CEBPA^{single-mut} genotype (data not shown). The MPO-positivity rate was widely distributed in patients who had mutant *NPM1* without *FLT3*-ITD genotype (median 26, range 0–100) and other genotypes (median 31, range 0–100). Kruskal–Wallis test showed that a significant difference of the MPO-positivity rate among three groups ($P = 0.005$). When comparing the individual groups by Dunn's Multiple Comparisons post hoc test for each group, there was a significant difference only for patients with *CEBPA*^{double-mut} versus patients with other genotypes.

4 Discussion

While cytogenetic group is considered to be the primary prognostic indicator in AML, the percentage of MPO-positive blast cells could be used to predict the prognosis of patients with normal karyotypes [6]. In this study, we found that *CEBPA* gene mutational status has impact on the frequency of MPO expression: the patients with the *CEBPA* mutation genotype displayed a significantly higher percentage of cells expressing MPO than those with other genotypes ($P < 0.01$). The association was even more significant when analyzed without the *CEBPA*^{single-mut} carrying patient, suggesting that high blast MPO activity is related to double *CEBPA* mutations. Although the mutant *NPM1* without *FLT3*-ITD genotype has been reported to be associated with a favorable prognosis in AML patients, there was no relationship between this type of mutation and the percentage of blasts showing MPO expression.

It is not clear how the *CEBPA*^{double-mut} genotype enhances MPO activity in AML blasts. It has been shown

that the MPO enhancer contains a *CEBPA* site contributing to its functional activity [23, 24], suggesting that the MPO gene is a major target of C/EBP α . Since it has been shown that both N-terminal frame-shift mutant and C-terminal mutant do not show transcriptional activity [25], we first speculated that mutations of the *CEBPA* gene might lead to decreased MPO activity, which turned out to be wrong. AML1 is another gene that has been reported to participate in up-regulation of MPO gene [26]. An AML1 site was identified in upstream enhancer of the human MPO gene, which appears to be necessary for maximal stimulation of MPO promoter activity. In patients with AML with t(8;21), the translocation results in an in-frame fusion between 5 exons of the AM1 gene and essentially all of the ETO gene producing a chimeric protein [27]. This protein, AML1-ETO, acts as a negative dominant inhibitor of wild-type AML1 [28], which theoretically could lead to down-regulation of AML1 target genes, such as MPO gene. However, blasts with t(8;21) have been shown to display higher levels of MPO expression both in clinical samples and in vitro experiments [29, 30], suggesting that the transcriptional alterations caused by these mutations are complex. The upregulation of blast MPO activity seen in *CEBP/* α ^{double-mut} cases may be due to alterations in the gene expression profile, rather than a simple dominant negative effect of mutated CEBP/ α . Further experiments including investigation of transactivation potential of CEBP/ α mutants on MPO promoter is necessary to clarify this mechanism.

CEBPA mutations are associated with a relatively favorable outcome, and it was recently shown in a multi-variable analysis including cytogenetic risk and the

Table 3 Frequency of *FLT3*-ITD, *NPM1*, and *CEBPA* mutations by clinical characteristics in de novo AML cases with a normal karyotype

	<i>FLT3</i>		<i>P</i>	<i>NPM1</i>		<i>P</i>	<i>CEBPA</i>		<i>P</i>
	ITD (<i>n</i> = 11)	Other type (<i>n</i> = 49)		Mutation without <i>FLT3</i> -ITD (<i>n</i> = 13)	Other type (<i>n</i> = 47)		Double mutation without <i>FLT3</i> -ITD (<i>n</i> = 8)	Other type (<i>n</i> = 52)	
Age			0.08			0.74			0.10
≤50	1	19		5	15		5	15	
>50	10	30		8	32		3	37	
PS			1.00			0.20			0.52
0–2	10	45		11	45		7	48	
3–4	1	4		2	2		1	4	
WBC			0.02			1.00			1.00
≤20,000	2	30		7	25		4	28	
>20,000	9	19		6	22		4	24	
FAB subtype			0.33			0.18			0.58
M1, M2, M4, M5	11	41		13	39		8	44	
M0, M6, M7	0	8		0	8		0	8	
JALSG score ^a			0.79			0.72			0.09
Favorable	0	5		0	5		2	3	
Intermediate	2	18		5	15		5	15	
Adverse	2	9		2	9		0	11	
CR ^a			1.00			0.56			0.56
Achievement	4	27		7	24		7	24	
Failure	0	5		0	5		0	5	

^a Analysis was carried in 36 patients with intensive chemotherapy

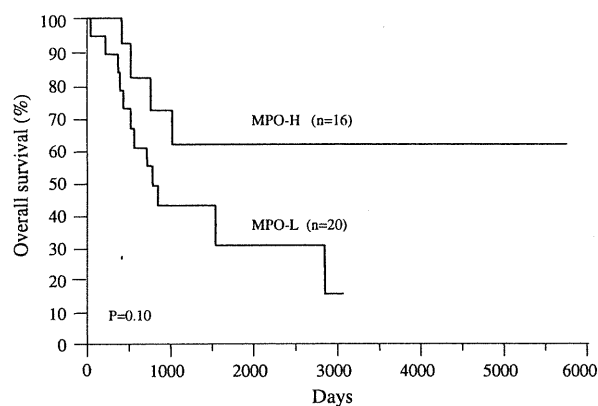


Fig. 3 Kaplan–Meier estimates of the probability of overall survival in 36 patients who received intensive chemotherapy, according to the percentage of myeloperoxidase-positive blasts. MPO-H (MPO-positive blasts: >50%) tended to have a positive effect on overall survival compared with MPO-L (MPO-positive blasts: ≤50%), although the difference was not statistically significant. The statistical significance of differences was evaluated with the log-rank test

FLT3-ITD and *NPM1* mutations that the *CEBPA*^{double-mut} genotype is associated with favorable overall and event-free survival [15, 16]. In a cohort of 60 cases of adult de novo AML, we identified 1 *CEBPA*^{single-mut} case and 10 *CEBPA*^{double-mut} cases, and in line with previous reports,

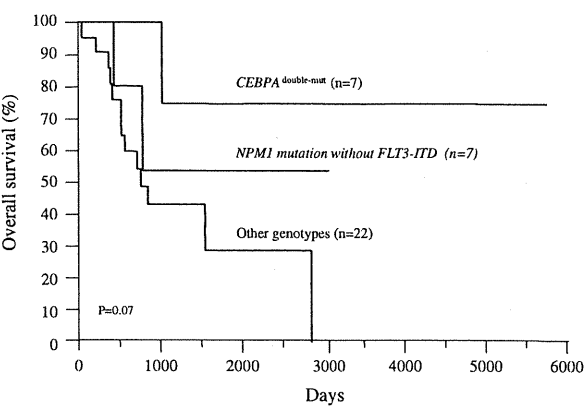
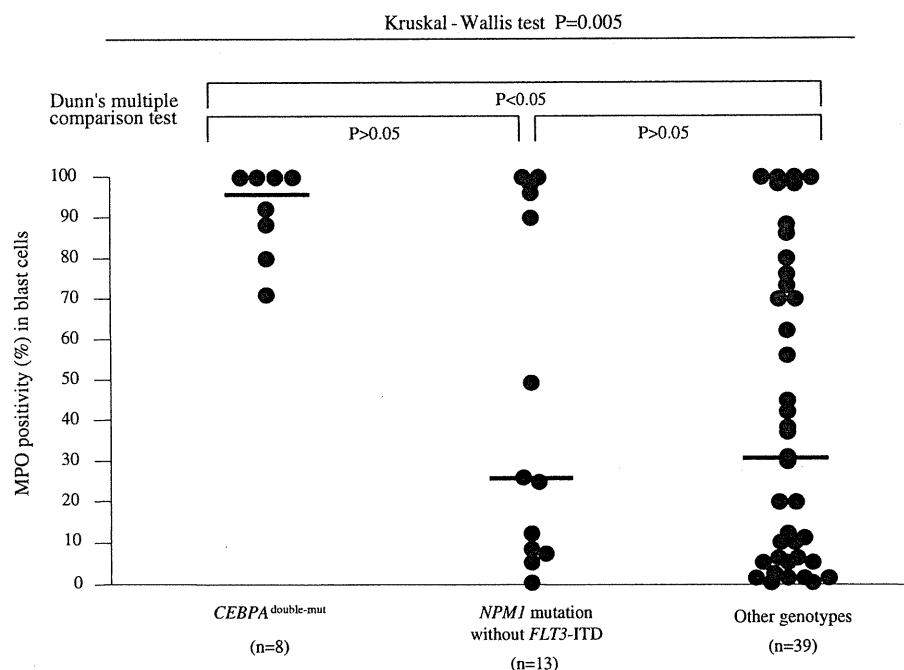


Fig. 4 Overall survival according to genotype in patients administered intensive chemotherapy. ‘Other genotypes’ was defined as the *FLT3*-ITD genotype, the *CEBPA*^{single-mut} genotype, and the triple-negative genotype consisting of the wild-type *NPM1* and *CEBPA* genotypes without *FLT3*-ITD. The patients with the *CEBPA*^{double-mut} genotype tended to show higher overall survival compared with the patients with ‘other genotypes’ (*P* = 0.07)

our study tended to show better overall survival in *CEBPA*^{double-mut} cases compared to cases with wild-type *CEBPA* in patients treated with intensive chemotherapy. We failed to find a prognostic effect in relation to the *CEBPA*^{double-mut} in patients treated with low dose

Fig. 5 MPO-positivity rate in blast according to genetic abnormalities in de novo AML patients with a normal karyotype. 'Other genotypes' was defined as the *FLT3*-ITD genotype, the *CEBPA*^{single-mut} genotype, and the triple-negative genotype consisting of the wild-type *NPM1* and *CEBPA* genotypes without *FLT3*-ITD. The median MPO-positivity rate (horizontal line) was significantly different between the *CEBPA*^{double-mut} genotype and 'other genotypes' (Kruskal–Wallis test followed by Dunn's multiple comparisons test: $P < 0.05$)



chemotherapy (data not shown), suggesting that the standard chemotherapy dose is necessary to improve the outcome of *CEBPA*^{double-mut} cases.

It is unclear why *CEBPA*^{double-mut} AML patients have a better outcome than those with *CEBPA* wild-type AML. One explanation is that high MPO expression leads to increased sensitivity to chemotherapeutic agents, such as to Ara-C [8]. To test this hypothesis, we also examined the association between blast MPO positivity and overall survival in *CEBPA* wild-type cases. Unexpectedly, when the patients were treated with intensive chemotherapy, the percentage of MPO-positive blasts was not significantly associated with overall survival in this group (data not shown), suggesting that the level of MPO expression itself is not responsible for the improvement in overall survival. However, as this analysis only involved 28 cases, we need to increase the number of cases in order to draw a definitive conclusion.

In summary, the data presented here suggested that the *CEBPA*^{double-mut} genotype was associated with high MPO blast activity in patients with a normal karyotype. Although the results were obtained from a single institution, the presence of *CEBPA*^{double-mut} genotype in high MPO group could explain, at least in part, why high MPO blast activity is associated with better overall survival. Further studies in a larger cohort of patients are necessary to assess blast MPO activity as a prognostic factor, especially in *CEBPA* wild-type patients with a normal karyotype.

Acknowledgments We would like to thank Dr. T Matsuo for his support, also Ms. N. Shirahama and Ms. M. Yamaguchi for their

assistance. This work was supported in part by grant from the Ministry of Health, Labor and Welfare and Ministry of Education, Culture, Sports, Science and Technology of Japan.

Conflict of interest All authors have no conflict of interest to report.

References

1. Miyawaki S, Sakamaki H, Ohtake S, Emi N, Yagasaki F, Mitani K, et al. A randomized, postremission comparison of four courses of standard-dose consolidation therapy without maintenance therapy versus three courses of standard-dose consolidation with maintenance therapy in adults with acute myeloid leukemia. *Cancer*. 2005;104:2726–34.
2. David G, Helen W, Fiona O, Keith W, Christine H, Georgina H, et al. The importance of diagnostic cytogenetics on outcome in AML: analysis of 1, 612 patients entered into the MRC AML 10 trial. *Blood*. 1998;92:2322–33.
3. Ohtake S, Miyawaki S, Fujita H, Kiyoi H, Shinagawa K, Usui N, et al. Randomized study of induction therapy comparing standard-dose idarubicin with high-dose daunorubicin in adult patients with previously untreated acute myeloid leukemia: JALSG AML201 Study. *Blood*. 2011;117:2358–65.
4. Bennett JM, Catovsky D, Daniel MT, Flandrin G, Galton DA, Gralnick HR, et al. Proposed revised criteria for the classification of acute myeloid leukemia. A report of the French–American–British Cooperative Group. *Ann Intern Med*. 1985;103:620–5.
5. World Health Organization. Classification of tumors. In: Jaffe ES, Harris NL, Stein H, Vardimann JW, editors. *Pathology and genetics of tumors of haematopoietic and lymphoid tissues*. Lyon: IARC Press; 2001. p. 79–80.
6. Matsuo T, Kuriyama K, Miyazaki Y, Yoshida S, Tomonaga M, Emi N, et al. The percentage of myeloperoxidase-positive blast

- cells is a strong independent prognostic factor in acute myeloid leukemia, even in the patients with normal karyotype. *Leukemia*. 2003;17:1538–43.
7. Taguchi J, Miyazaki Y, Tsutsumi C, Sawayama Y, Ando K, Tsushima H, et al. Expression of the myeloperoxidase gene in AC133 positive leukemia cells relates to the prognosis of acute myeloid leukemia. *Leuk Res*. 2006;30:1105–12.
 8. Sawayama Y, Miyazaki Y, Ando K, Horio K, Tsutsumi C, Tsushima H, et al. Expression of myeloperoxidase enhances the chemosensitivity of leukemia cells through the generation of reactive oxygen species and the nitration of protein. *Leukemia*. 2008;22:956–64.
 9. Schnittger S, Schoch C, Kern W, Mecucci C, Tschulik C, Martelli MF, et al. Nucleophosmin gene mutations are predictors of favorable prognosis in acute myelogenous leukemia with a normal karyotype. *Blood*. 2005;106:3733–9.
 10. Boissel N, Renneville A, Biggio V, Philippe N, Thomas X, Cayuela JM, et al. Prevalence clinical profile, and prognosis of NPM mutations in AML with normal karyotype. *Blood*. 2005;106:3618–20.
 11. Yanada M, Matsuo K, Suzuki T, Kiyoi H, Naoe T. Prognostic significance of FLT3 internal tandem duplication and tyrosine kinase domain mutations for acute myeloid leukemia: a meta-analysis. *Leukemia*. 2005;19:1345–9.
 12. Preudhomme C, Sagot C, Boissel N, Cayuela JM, Tigaud I, de Botton S, et al. Favorable prognostic significance of CEBPA mutations in patients with de novo acute myeloid leukemia: a study from the Acute Leukemia French Association (ALFA). *Blood*. 2002;100:2717–23.
 13. Gombart AF, Hofmann WK, Kawano S, Takeuchi S, Krug U, Kwok SH, et al. Mutations in the gene encoding the transcription factor CCAAT/enhancer binding protein alpha in myelodysplastic syndromes and acute myeloid leukemias. *Blood*. 2002;99:1332–40.
 14. Schlenk RF, Döhner K, Krauter J, Fröhling S, Corbacioglu A, Bullinger L, et al. Mutations and treatment outcome in cytogenetically normal acute myeloid leukemia. *N Engl J Med*. 2008;358:1909–18.
 15. Wouters BJ, Löwenberg B, Erpelinck-Verschueren CA, van Putten WL, Valk PJ, Delwel R. Double CEBPA mutations, but not single CEBPA mutations, define a subgroup of acute myeloid leukemia with a distinctive gene expression profile that is uniquely associated with a favorable outcome. *Blood*. 2009;113:3088–91.
 16. Dufour A, Schneider F, Metzeler KH, Hoster E, Schneider S, Zellmeier E, et al. Acute myeloid leukemia with biallelic CEBPA gene mutations and normal karyotype represents a distinct genetic entity associated with a favorable clinical outcome. *J Clin Oncol*. 2010;28:570–7.
 17. Miyawaki S, Kobayashi T, Tanimoto M, Kuriyama K, Murakami H, Yoshida M, et al. Comparison of leucopenia between cytarabine and behenoyl cytarabine in JALSG AML-89 consolidation therapy. The Japan Adult Leukemia Study Group. *Int J Hematol*. 1999;70:56–7.
 18. Miyawaki S, Tanimoto M, Kobayashi T, Minami S, Tamura J, Omoto E, Kuriyama K, et al. No beneficial effect from addition of etoposide to daunorubicin, cytarabine, and 6-mercaptopurine in individualized induction therapy of adult acute myeloid leukemia: the JALSG-AML92 study. Japan Adult Leukemia Study Group. *Int J Hematol*. 1999;70:97–104.
 19. Ohtake S, Miyawaki S, Kiyoi H, Miyazaki Y, Okumura H, Matsuda S, Nagai T, et al. Randomized trial of response-oriented individualized versus fixed-schedule induction chemotherapy with idarubicin and cytarabine in adult acute myeloid leukemia: the JALSG AML95 study. *Int J Hematol*. 2010;91:276–83.
 20. Kiyoi H, Naoe T, Nakano Y, Yokota S, Minami S, Miyawaki S, et al. Prognostic implication of FLT3 and N-RAS gene mutations in acute myeloid leukemia. *Blood*. 1999;93:3074–80.
 21. Falini B, Mecucci C, Tiacci E, Alcalay M, Rosati R, Pasqualucci L, et al. Cytoplasmic nucleophosmin in acute myelogenous leukemia with a normal karyotype. *N Engl J Med*. 2005;352:254–66.
 22. Kaplan E, Meier P. Nonparametric estimation from incomplete observations. *J Am Stat Assoc*. 1958;53:457–62.
 23. Yao C, Qin Z, Works KN, Austin GE, Young AN. CEBP and C-Myb sites are important for the functional activity of the human myeloperoxidase upstream enhancer. *Biochem Biophys Res Commun*. 2008;371:309–14.
 24. Reckzeh K, Cammenga J. Molecular mechanisms underlying deregulation of C/EBP α in acute myeloid leukemia. *Int J Hematol*. 2010;91:557–68.
 25. Kato N, Kitamura J, Doki N, et al. Two types of C/EBP α mutations play distinct but collaborative roles in leukemogenesis: lessons from clinical data and BMT models. *Blood*. 2011;117:221–33.
 26. Austin GE, Zhao WG, Regmi A, Lu JP, Braun J. Identification of an upstream enhancer containing an AML1 site in the human myeloperoxidase (MPO) gene. *Leuk Res*. 1998;22:1037–48.
 27. Erickson PF, Robinson M, Owens G, Drabkin HA. The ETO portion of acute myeloid leukemia t(8;21) fusion transcript encodes a highly evolutionarily conserved, putative transcription factor. *Cancer Res*. 1994;54:1782–6.
 28. Meyers S, Lenny N, Hiebert SW. The t(8;21) fusion protein interferes with AML-1B-dependent transcriptional activation. *Mol Cell Biol*. 1995;15:1974–82.
 29. Khoury H, Dalal BI, Nantel SH, Horsman DE, Lavoie JC, Shepherd JD, et al. Correlation between karyotype and quantitative immunophenotype in acute myelogenous leukemia with t(8;21). *Modern Pathol*. 2004;17:1211–6.
 30. Shimada H, Ichikawa H, Ohki M. Potential involvement of the AML1-MTG8 fusion protein in the granulocytic maturation characteristic of the t(8;21) acute myelogenous leukemia revealed by microarray analysis. *Leukemia*. 2002;16:874–85.

Clinical Cancer Research



Pulmonary Inflammatory Myofibroblastic Tumor Expressing a Novel Fusion, PPFIBP1 –ALK: Reappraisal of Anti-ALK Immunohistochemistry as a Tool for Novel ALK Fusion Identification

Kengo Takeuchi, Manabu Soda, Yuki Togashi, et al.

Clin Cancer Res 2011;17:3341-3348. Published OnlineFirst March 23, 2011.

Updated Version

Access the most recent version of this article at:
doi:10.1158/1078-0432.CCR-11-0063

Supplementary Material

Access the most recent supplemental material at:
<http://clincancerres.aacrjournals.org/content/suppl/2011/05/19/1078-0432.CCR-11-0063.DC1.html>

Cited Articles

This article cites 43 articles, 20 of which you can access for free at:
<http://clincancerres.aacrjournals.org/content/17/10/3341.full.html#ref-list-1>

E-mail alerts

Sign up to receive free email-alerts related to this article or journal.

Reprints and Subscriptions

To order reprints of this article or to subscribe to the journal, contact the AACR Publications Department at pubs@aacr.org.

Permissions

To request permission to re-use all or part of this article, contact the AACR Publications Department at permissions@aacr.org.

Pulmonary Inflammatory Myofibroblastic Tumor Expressing a Novel Fusion, PPFIBP1-ALK: Reappraisal of Anti-ALK Immunohistochemistry as a Tool for Novel ALK Fusion Identification

Kengo Takeuchi^{1,2}, Manabu Soda⁴, Yuki Togashi^{1,2}, Emiko Sugawara^{1,5}, Satoko Hatano^{1,2}, Reimi Asaka^{1,2}, Sakae Okumura³, Ken Nakagawa³, Hiroyuki Mano^{4,6}, and Yuichi Ishikawa²

Abstract

Purpose: The anaplastic lymphoma kinase (ALK) inhibitor crizotinib has been used in patients with lung cancer or inflammatory myofibroblastic tumor (IMT), both types harboring ALK fusions. However, detection of some ALK fusions is problematic with conventional anti-ALK immunohistochemistry because of their low expression. By using sensitive immunohistochemistry, therefore, we reassessed "ALK-negative" IMT cases defined with conventional immunohistochemistry (approximately 50% of all examined cases).

Experimental Design: Two cases of ALK-negative IMT defined with conventional anti-ALK immunohistochemistry were further analyzed with sensitive immunohistochemistry [the intercalated antibody-enhanced polymer (iAEP) method].

Results: The two "ALK-negative" IMTs were found positive for anti-ALK immunohistochemistry with the iAEP method. 5'-rapid amplification of cDNA ends identified a novel partner of ALK fusion, protein-tyrosine phosphatase, receptor-type, F polypeptide-interacting protein-binding protein 1 (PPFIBP1) in one case. The presence of PPFIBP1-ALK fusion was confirmed with reverse transcriptase PCR, genomic PCR, and FISH. We confirmed the transforming activities of PPFIBP1-ALK with a focus formation assay and an *in vivo* tumorigenicity assay by using 3T3 fibroblasts infected with a recombinant retrovirus encoding PPFIBP1-ALK. Surprisingly, the fusion was also detected by FISH in the other case.

Conclusions: Sensitive immunohistochemical methods such as iAEP will broaden the potential value of immunohistochemistry. The current ALK positivity rate in IMT should be reassessed with a more highly sensitive method such as iAEP to accurately identify those patients who might benefit from ALK-inhibitor therapies. Novel ALK fusions are being identified in various tumors in addition to IMT, and thus a reassessment of other "ALK-negative" cancers may be required in the forthcoming era of ALK-inhibitor therapy. *Clin Cancer Res*; 17(10); 3341–8. ©2011 AACR.

Introduction

Anaplastic lymphoma kinase (ALK) is a receptor tyrosine kinase that was discovered in anaplastic large cell lymphoma (ALCL) in the form of a fusion protein, NPM-ALK. (1, 2). In addition to ALCL (fused to NPM, TPM3, TPM4, ATIC, TFG, CLTC, MSN, MYH9, or ALO17; refs. 1–10), ALK

has further been found to generate fusions in inflammatory myofibroblastic tumor (IMT; TPM3, TPM4, CLTC, CARS, RANBP2, ATIC, or SEC31L1; refs. 10–15), ALK-positive large B-cell lymphoma (CLTC, NPM, SEC31L1, or SQSTM1; 16–19), lung cancer (EML4 or KIF5B; refs. 20, 21), and ALK-positive histiocytosis (TPM3; ref. 22). Besides, some ALK fusions have been reported without showing histopathologic evidence: TPM4-ALK in esophageal squamous cell carcinoma (23, 24), TFG-ALK in lung adenocarcinoma (25), and EML4-ALK in colon and breast carcinomas (26). The wild-type ALK is mainly expressed in the developing nervous system, and is usually not expressed in other normal tissues (27). A fusion protein formation with a partner through chromosomal translocations is the most common mechanism of ALK overexpression and ALK kinase domain activation. These features render ALK fusion onco-kinase an ideal molecular target.

Recently, the ALK inhibitor crizotinib has been used in patients with lung cancer or IMT, both types harboring ALK fusions (28, 29). The compound showed a 57% response rate in lung cancers (28), and a strong response for several months in IMT (29). Crizotinib and other ALK inhibitors

Authors' Affiliations: ¹Pathology Project for Molecular Targets; ²Division of Pathology; and ³Department of Thoracic Surgical Oncology, Thoracic Center, Cancer Institute Hospital, Japanese Foundation for Cancer Research, Tokyo; ⁴Division of Functional Genomics, Jichi Medical University, Tochigi; ⁵Department of Comprehensive Pathology, Graduate School, Tokyo Medical and Dental University; and ⁶Department of Medical Genomics, Graduate School of Medicine, University of Tokyo, Tokyo, Japan

Note: Supplementary data for this article are available at Clinical Cancer Research Online (<http://clincancerres.aacrjournals.org/>).

Corresponding Author: Kengo Takeuchi, Pathology Project for Molecular Targets, The Cancer Institute, Japanese Foundation for Cancer Research, Tokyo 135-8550, Japan. Phone: +8133-520-0111; Fax: +8133-570-0230; E-mail: kentakeuchi-tyk@umin.net

doi: 10.1158/1078-0432.CCR-11-0063

©2011 American Association for Cancer Research.

Translational Relevance

Anaplastic lymphoma kinase (ALK) inhibitors have become one of the most promising groups of molecularly targeted drugs. Therefore, ALK is no longer a mere research target or simply a diagnostic marker, but is directly linked to the therapeutic benefit of patients harboring the fusions.

Pathologic diagnoses for ALK fusion-positive tumors have been made reliably with anti-ALK immunohistochemistry. Since the discovery of EML4-ALK, however, an unexpected problem in anti-ALK immunohistochemistry has become apparent, that is, the inability to detect a low level of EML4-ALK expression. To overcome this, we developed the intercalated antibody-enhanced polymer immunohistochemistry, which successfully detected EML4-ALK.

In other words, this indicates that unknown ALK fusions, particularly those expressed at a low level, may wait to be discovered in "ALK-negative" tumors defined with conventional immunohistochemistry. In the forthcoming era of ALK-inhibitor therapy, "ALK-negative" tumors should be reassessed with a high sensitive immunohistochemistry and, if positive, be further examined with appropriate molecular method(s).

have thus become one of the most promising groups of molecularly targeted drugs. Therefore, the sensitive and accurate identification of ALK fusion in tumors has also become clinically relevant, because it is no longer a mere research target or simply a diagnostic marker, but is directly linked to the therapeutic benefit of patients harboring the fusions.

Identification of such ALK fusions, especially within ALCL, has been prompted by the immunohistochemical staining pattern with antibodies to ALK. In ALCL, the most common ALK fusion is NPM-ALK (comprising approximately 80% of all cases), and its immunohistochemical staining pattern is both nuclear and cytoplasmic. NPM has a nuclear localization signal in the C-terminal region, and therefore the heterodimers of wild-type NPM with NPM-ALK fusion protein are transported to the nucleus whereas NPM-ALK homodimers remain within the cytoplasm (30). In contrast, other fusions do not localize in the nucleus and do not show a nuclear staining pattern in anti-ALK immunohistochemistry. Interestingly, each ALK fusion usually has its own characteristic anti-ALK immunohistochemical staining pattern, because the subcellular localization of ALK fusions is dependent on the corresponding fusion partners. Anti-ALK immunohistochemistry has thus become a highly useful tool for both research and diagnostic purposes.

Since the discovery of EML4-ALK fusion in lung cancer (20), however, an unexpected problem in anti-ALK immunohistochemistry has become apparent, that is, the inability to detect a low level of fusion expression. To overcome this, we developed the intercalated antibody-enhanced

polymer (iAEP) method, which moderately raises sensitivity in the immunohistochemical detection system (21). With this very simple method, anti-ALK immunohistochemistry has become a potent weapon in the diagnosis of EML4-ALK-positive lung cancer (21, 31–33). Other researchers used an anti-ALK rabbit monoclonal antibody, which is usually more sensitive than mouse monoclonal antibody, which can stain EML4-ALK (34). However, most EML4-ALK-positive lung cancer tissues do not stain well with conventional anti-ALK immunohistochemical methods because of the low message/protein level of EML4-ALK (21, 35). The expression level of a fusion gene depends on the promoter activity of the 5'-side gene, and that of EML4 is likely to be lower than that of the other ALK fusion partner genes, which may explain why EML4-ALK had not been discovered until 12 years after the development of the first anti-ALK antibody became available for immunohistochemistry (36). In other words, a tumor that immunostains for ALK only by a sensitive immunohistochemistry method may harbor a novel ALK fusion. Interestingly, in this study, we detected 2 IMT cases positive for ALK immunohistochemistry only when stained by iAEP method (21), and successfully identified a novel fusion gene, protein-tyrosine phosphatase, receptor-type, F polypeptide-interacting protein-binding protein 1 (PPFIBP1)-ALK.

Materials and Methods

Materials

Pathologic specimens from 2 pulmonary IMT cases, originally diagnosed as fibrous histiocytoma (1988: case 1, 45-year-old male; 1998: case 2, 34-year-old female), were reassessed morphologically and immunohistochemically. Surgically removed tumor specimens were routinely fixed in 20% neutralized formalin and embedded in paraffin for conventional histopathologic examination. For case 2, total RNA was extracted from the corresponding snap-frozen specimen and purified with the use of an RNeasy Mini kit (Qiagen). The study was approved by the institutional review board of the Japanese Foundation for Cancer Research.

Immunohistochemistry

Formalin-fixed, paraffin-embedded tissue was sliced at a thickness of 4 μ m, and the sections were placed on silane-coated slides. For antigen retrieval, the slides were heated for 40 min at 97°C in Target Retrieval Solution (pH 9.0; Dako). For the conventional staining procedure, the slides were incubated at room temperature with Protein Block Serum-free Ready-to-Use solution (Dako) for 10 minutes and then with primary antibodies against ALK (5A4), smooth muscle actin, muscle-specific actin (HHF35), CD34, cytokeratins (AE1/AE3), S100, or desmin for 30 minutes. The immune complexes were then detected with dextran polymer reagent (EnVision + DAB system; Dako) and an AutoStainer instrument (Dako). The iAEP method was also used for the sensitive detection of ALK, as described previously (21).

Isolation of PPFIBP1-ALK fusion

To obtain cDNA fragments corresponding to a novel *ALK* fusion gene, we used a 5'-RACE method with the SMART RACE cDNA Amplification Kit (Clontech) according to the manufacturer's instructions, with a minor modification: the ALK2458R primer (5'-GTAGTTGGGGTTGTAGTCGGT-CATGATGGT-3') was used as the gene-specific reverse primer.

From the oligo(dT)-primed cDNA obtained from case 2 RNA, a 471bp cDNA fragment containing the fusion point was specifically amplified with the primers PPFIBP1-592F (5'-AGAGACACAGAGGGGCTGATT-3') and ALK3078RR (5'-ATCCAGTTCGTCCTGTTCAGAGC-3').

PCR analysis of genomic DNA for *PPFIBP1-ALK* in case 2 was carried out with a pair of primers flanking the putative fusion point, PPFIBP1-607F (5'-CTGATTCAGGAGATCA-ATGATTGAGGT-3') and Fusion-RT-AS (5'-TCTTGCCAG-CAAAGCAGTAGTTGG-3').

From the cDNA, a full-length cDNA for *PPFIBP1-ALK* was amplified by PCR with the PA-w-cDNA-in-S primer (5'-TATCTGGGTTGGAATTTGCCCCCTG-3') and the KA-w-cDNA-in-AS primer (5'-TGAGTGTGCGACCGAGCTCAGG-3') and PrimeSTAR HS DNA polymerase (TakaraBio).

FISH

FISH analysis of gene fusion was carried out with bacterial artificial chromosome (BAC) clone-derived DNA probes for *ALK* and *PPFIBP1*. Unstained sections (4 μ m thick) were subjected to hybridization with an *ALK*-split probe set (Abbott) or BAC clone-derived probes for *ALK* (RP11-984121, RP11-62B19) and *PPFIBP1*

(RP11-1060J15). Hybridized slides were then stained with DAPI and examined with the fluorescence microscope BX51 (Olympus).

Transformation assay for ALK fusion proteins

Analysis of the transforming activity of PPFIBP1-ALK was carried out as described previously (20, 37, 38). Briefly, the pMXS-based expression plasmid for PPFIBP1-ALK, EML4-ALK variant 1, or NPM-ALK was used to generate recombinant ecotropic retrovirus, followed by individual infection of mouse 3T3 fibroblasts (39). Formation of the transformed foci was evaluated after culturing the cells for 14 days. The same set of 3T3 cells was subcutaneously injected into nu/nu mice, and tumor formation was examined after 20 days. The animal experiments were approved by the animal ethics committee of Jichi Medical University.

Results

Morphology and immunophenotype of PPFIBP1-ALK-positive IMT

Histopathologic analysis of the 2 IMT cases revealed a marked proliferation of cells composed of somewhat histiocytoid spindle cells showing a fascicular or storiform pattern. The tumor cells were uniform and had pale eosinophilic cytoplasm and an oval vesicular nucleus, within which a small nucleolus was centrally located. Mild inflammatory infiltrate containing lymphocytes, plasma cells, foamy histiocytes, and multinucleated giant cells was observed (Fig. 1A and 1D). The immunophenotype of the 2 cases was negative for smooth muscle actin,

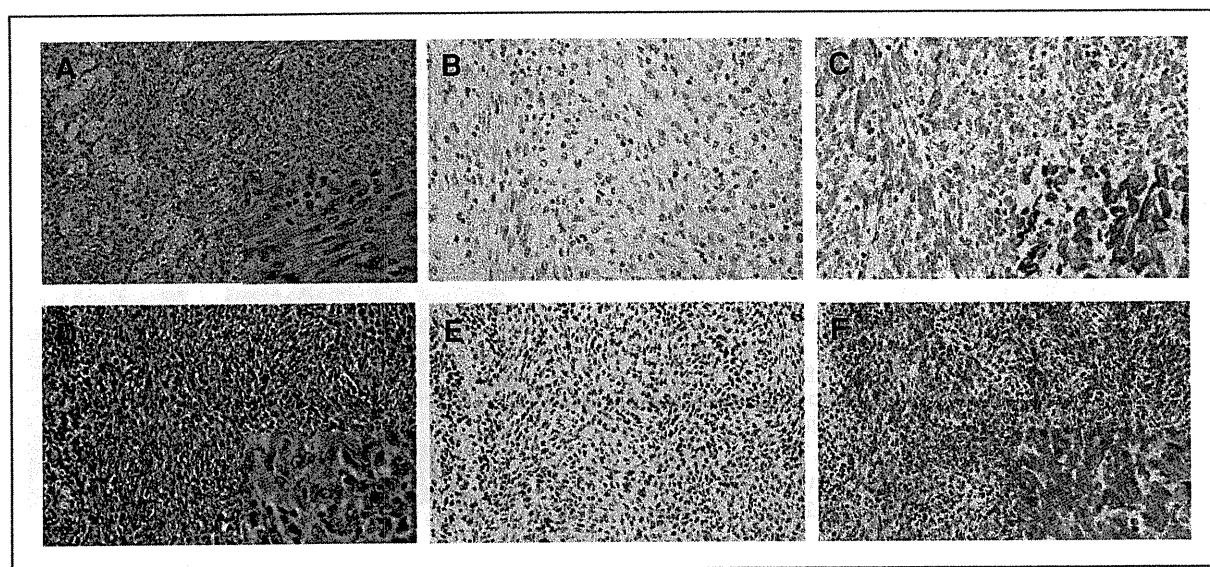


Figure 1. Histopathology of PPFIBP1-ALK-positive IMT. Diffuse proliferation of histiocytoid spindle cells showing a fascicular or storiform pattern. The tumor cells were uniform and had pale eosinophilic cytoplasm and an oval vesicular nucleus, within which a small nucleolus was centrally located. Mild inflammatory infiltrate containing lymphocytes, plasma cells, and foamy histiocytes is observed (A and D). The tumor cells were negative for ALK with conventional anti-ALK immunohistochemistry (B and E), but were clearly positive for ALK when the iAEP method was used. The staining pattern is diffuse cytoplasmic (C and F). Case 1 (A-C), Case 2 (D-F).

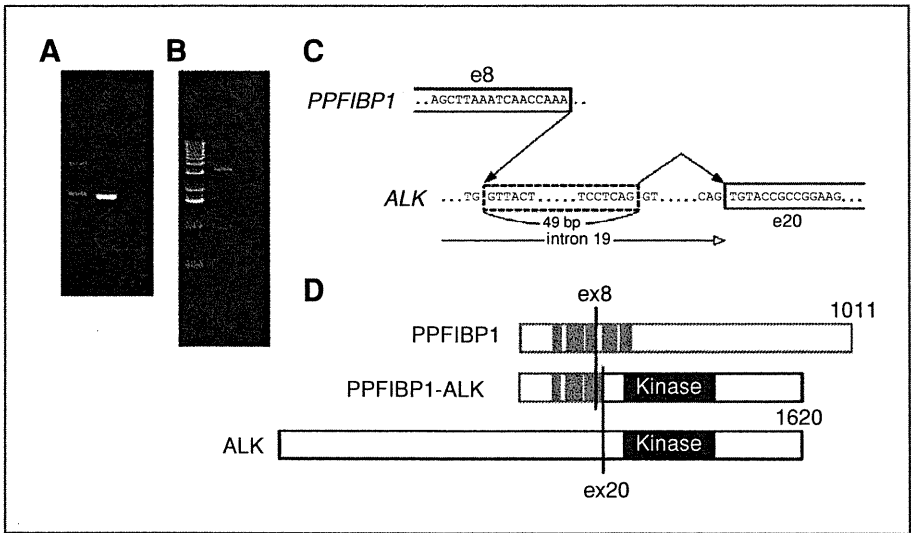


Figure 2. Identification of PPFIBP1-ALK: a PCR product of 471 bp covering the fusion point of *PPFIBP1*-*ALK* cDNA was specifically amplified from the tumor cells of case 2. The left lane contains DNA size standards (100 bp ladder). The right lane represents no template control (A). A PCR product of approximately 3 kbp covering the genomic fusion point of *PPFIBP1*-*ALK* was specifically amplified from the tumor cells of case 2. The left lane contains DNA size standards (1 kbp ladder). The right lane represents no template control (B). In our 5'-RACE products, exon 8 of *PPFIBP1* cDNA was fused to a 49 bp sequence in intron 19 of *ALK*, followed by exon 20 of *ALK* (C). *PPFIBP1* contains 5 coiled-coil domains. A chromosome translocation, t(2;10)(p23;p11), generates a fusion protein in which the top 3 coiled-coil domains of *PPFIBP1* and the intracellular region of *ALK* (containing the tyrosine kinase domain) are conserved. Numbers indicate amino acid positions of each protein (D).

HHF35, CD34, AE1/AE3, and S100. Desmin was focally positive in case 1, but was negative in case 2.

Identification of PPFIBP1-ALK as a novel ALK fusion gene

We conducted anti-ALK immunohistochemistry on 2 morphologically typical pulmonary IMT cases, originally diagnosed as fibrous histiocytoma. Immunostaining for ALK with the conventional polymer method led to the revised diagnosis of "ALK-negative" IMT (Fig. 1B and E). In the present study, anti-ALK immunohistochemistry with the iAEP method, however, showed a diffuse positive cytoplasmic staining (Fig. 1C and F), indicating the possibility of ALK fusion to a novel partner gene, the expression level of which is modest. To address this issue, in case 2 we conducted 5'-RACE assay for the isolation of an upstream cDNA to the ALK kinase domain cDNA, for which snap-frozen material was available.

Interestingly, we isolated a cDNA fragment containing exon 8 of *PPFIBP1* followed by a 49 bp-sequence within intron 19 of *ALK* and coupled to exon 20 of *ALK* (Fig. 2), suggesting the presence of a novel fusion between *PPFIBP1* and *ALK* genes. Because insertion of the intronic 49 bp allows an in-frame fusion between the 2 genes, this rearrangement likely produces a novel fusion-type tyrosine kinase. To confirm the genomic rearrangement responsible for the *PPFIBP1*-*ALK* fusion, a genomic PCR assay (Fig. 2B) and both *ALK* split and *PPFIBP1*-*ALK* fusion FISH assays (Fig. 3) were carried out. All results were consistent with the presence of t(2;12)(p23;p11) leading to the generation of *PPFIBP1*-*ALK*. Owing to the limited material available in

case 1, only the FISH analyses were carried out. Surprisingly, these results also indicate the presence of *PPFIBP1*-*ALK* (Fig. 3, Supplementary Fig. 2A-C).

Transforming activities of PPFIBP1-ALK

To prove that the t(2;12)(p23;p11) rearrangement leads to the production of *PPFIBP1*-*ALK* kinase, in case 2 we attempted to amplify from the cDNA a full-length cDNA encoding the protein. By using a sense primer at the 5'-untranslated region of *PPFIBP1* mRNA (GenBank accession no. NM_003622) and an antisense primer at

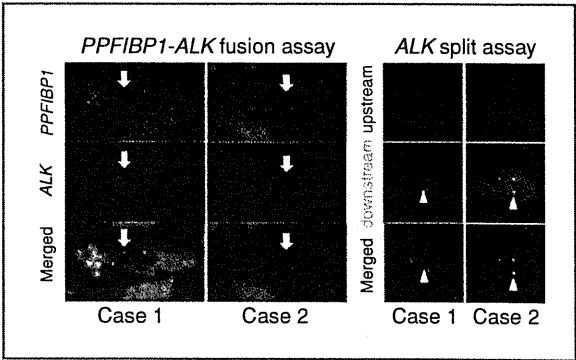


Figure 3. FISH analyses for *PPFIBP1*-*ALK*: sections of tumors positive for *PPFIBP1*-*ALK* were subjected to FISH analyses. In *PPFIBP1*-*ALK* fusion assays (left) the fusion genes are indicated by arrows. In *ALK* split assays (right) the 3'-sides of *ALK* are indicated by arrowheads. The color of fluorescence for the BAC clones and the case numbers in each hybridization are indicated. Nuclei are stained blue with DAPI.